2016

REFERENCE POINT INDENTATION OF HUMAN TRABECULAR BONE TREATED WITH BISPHOSPHONATES FOR VARYING DURATIONS

Drew Jones
University of Kentucky, daj349@gmail.com
Digital Object Identifier: http://dx.doi.org/10.13023/ETD.2016.370

STUDENT AGREEMENT:

I represent that my thesis or dissertation and abstract are my original work. Proper attribution has been given to all outside sources. I understand that I am solely responsible for obtaining any needed copyright permissions. I have obtained needed written permission statement(s) from the owner(s) of each third-party copyrighted matter to be included in my work, allowing electronic distribution (if such use is not permitted by the fair use doctrine) which will be submitted to UKnowledge as Additional File.

I hereby grant to The University of Kentucky and its agents the irrevocable, non-exclusive, and royalty-free license to archive and make accessible my work in whole or in part in all forms of media, now or hereafter known. I agree that the document mentioned above may be made available immediately for worldwide access unless an embargo applies.

I retain all other ownership rights to the copyright of my work. I also retain the right to use in future works (such as articles or books) all or part of my work. I understand that I am free to register the copyright to my work.

REVIEW, APPROVAL AND ACCEPTANCE

The document mentioned above has been reviewed and accepted by the student's advisor, on behalf of the advisory committee, and by the Director of Graduate Studies (DGS), on behalf of the program; we verify that this is the final, approved version of the student's thesis including all changes required by the advisory committee. The undersigned agree to abide by the statements above.

Drew Jones, Student

Dr. David Pienkowski, Major Professor

Dr. Abhijit Patwardhan, Director of Graduate Studies

REFERENCE POINT INDENTATION OF HUMAN TRABECULAR BONE TREATED WITH BISPHOSPHONATES FOR VARYING DURATIONS

THESIS

A thesis submitted in partial fulfillment of the requirements for the degree of Master of Science in Biomedical Engineering in the College of Engineering at the University of Kentucky

By

Drew Alexander Jones

Lexington, KY

Director: Dr. David Pienkowski, Professor of Biomedical Engineering

Lexington, KY

2016

ABSTRACT OF THESIS

REFERENCE POINT INDENTATION OF HUMAN TRABECULAR BONE TREATED WITH BISPHOSPHONATES FOR VARYING DURATIONS

Reference point indentation (RPI), a novel form of micro-indentation, quantifies RPI material parameters which correlate with modulus, yield stress, strength, or toughness. Information linking bisphosphonate treatment length with the material properties of osteoporotic trabecular bone is needed to improve patient treatment. The objectives of this study were to: 1) determine if RPI can be used to successfully evaluate human trabecular bone and if so, determine an optimized test method for using RPI on trabecular bone, and 2) use this method to determine if any RPI parameters are related to the duration of bisphosphonate treatment.

Indentation using a 4 N applied force for 5 cycles was determined to be optimal and used to indent trabecular bone samples from 44 post-menopausal, osteoporotic female patients treated with bisphosphonates for varying (0.8 to 14 years) durations.

Considering patient age and calcium supplementation use as covariates, six RPI parameters were significantly ($p<0.05$) related to BP treatment duration. These results show that the duration of BP treatment is associated with declining RPI-parameters in human trabecular bone. Given prior findings linking these RPI parameters with established material parameters, the present findings suggest that increasing duration of BP treatment is associated with declining trabecular bone material properties.

KEYWORDS: Reference Point Indentation, bisphosphonates, trabecular bone quality

Drew Jones

July 27th 2016

REFERENCE POINT INDENTATION OF HUMAN TRABECULAR BONE TREATED WITH BISPHOSPHONATES FOR VARYING DURATIONS

By

Drew Alexander Jones

Dr. David Pienkowski, Ph.D., M.B.A.
Director of Thesis

Dr. Abhijit Patwardhan, Ph.D.
Director of Graduate Studies

July, 27th 2016

TABLE OF CONTENTS

LIST OF TABLES

LIST OF FIGURES

1 Introduction

1.1 Bone

Bone is a composite material consisting of mineralized calcium, collagen fibers, water, and other proteins [1]. This mineralized form of calcium, known as hydroxyapatite, forms around collagen fibers [1]. Hydroxyapatite crystals grow in the same orientation as collagen fibers; this contributes to the anisotropic material properties of bone [1]. Mineralization provides strength and stiffness to bone while collagen provides flexibility and energy absorption [2].

The relative amounts of mineral and matrix in bone, commonly measured by the mineral/matrix ratio by using a variety of spectroscopic techniques, has a significant effect on the bone's elastic modulus, strength, and toughness (Figure 1.1) [2]. Hyper-mineralized bone has a higher elastic modulus but reduced toughness [2]. Hypo-mineralized bone has an increased toughness, a lower modulus, and an intermediate strength [2].

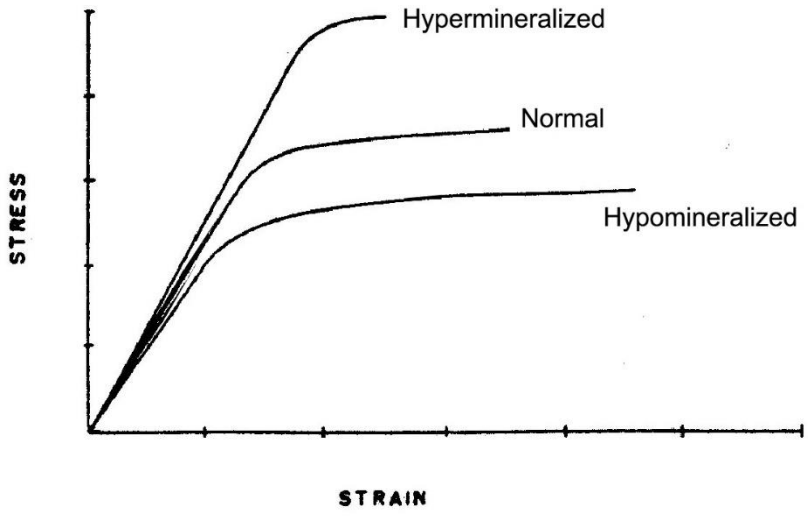

Figure 1.1 Bone Material Properties with Varying Mineralization

There are two distinctive types of human bone (Figure 1.2). Trabecular bone is a mesh-like network of thin, calcified tissue strands. Cortical bone is a thick, dense layer of calcified tissue formed as the outer shell of bone. Only 15-25% of trabecular bone is calcified while cortical bone is 80-90% calcified [1]. Both types have important load

bearing roles, but trabecular bone's high surface area to volume ratio also serves a significant role in calcium homeostasis [1].

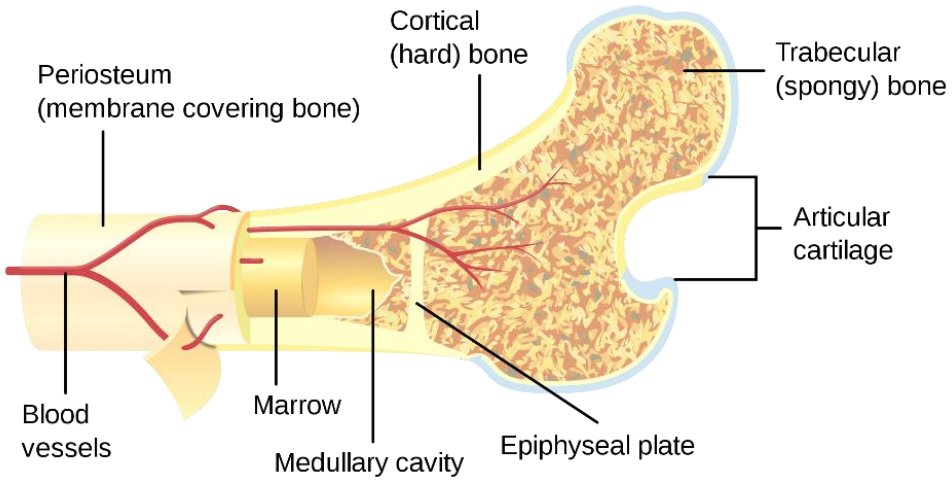

Figure 1.2 Parts of Bone

1.2 Osteoporosis

Osteoporosis is a bone disease characterized by an above-average increase in normal bone porosity and a below-average reduction in bone mineral density (BMD) [3]. This disease commonly occurs in post-menopausal Caucasian women due to an estrogen-deficient related increase in bone turnover and subsequent decrease in bone mineralization [4]. Estrogen modulates bone resorption by inducing osteoclast apoptosis and suppressing osteoclastogenic cytokine production [3]. Lower estrogen levels allow for increased osteoclast activity which results in increased turnover, hypomineralization, and mechanically disadvantageous microstructural characteristics such as fewer, thinner, and less well connected trabeculae (Figure 1.3).

Osteoporosis is diagnosed by measuring lumbar spine and proximal hip BMD using dual-energy x-ray absorptiometry [5]. The World Health Organization's criteria for osteoporosis is that if either hip or spine BMD is more than 2.5 standard deviations below the gender-specific population average BMD, then the patient is considered osteoporotic [5].

Osteoporosis is a major health problem because of the loss of adequate bone strength that occurs due to increased porosity, decreased cortical thickness, reduced trabecular bone structural parameters, and adverse material property changes that collectively render bone unable to withstand normal physiologically imposed loading. These structural and compositional changes to bone decrease the extrinsic strength of bone and have shown a stronger correlation with patient fracture risk than BMD [5] [6] [7] [8] [9].

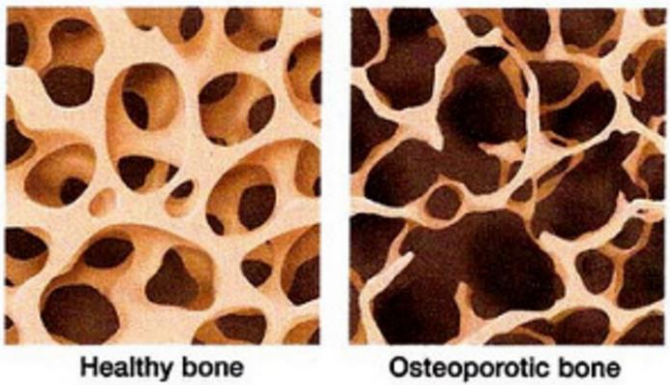

Figure 1.3 Healthy vs Osteoporotic Trabecular Bone

1.3 Osteoporosis Prevalence

Fractures are the most serious complication of osteoporosis [10]. Most osteoporotic fractures occur in the hip or spine and can result in permanent disability or initiate a sequence of downward-spiraling events that culminate in death [10]. An increasing number of women with post-menopausal osteoporosis, and the ensuing compromises to life quality as well as healthcare costs due to osteoporosis-related fractures, underscore the need for effective treatments. An estimated 10 million Americans were osteoporotic and an additional 34 million had low bone mass in 2011 [11]. Healthcare costs due to osteoporosis treatment and osteoporotic fractures were estimated to be $22 billion in 2008 alone [12]. These costs will grow because the number of Americans with osteoporosis is expected to increase to more than 14 million by 2020 [11] [12] [4].

1.4 Treatments for Osteoporosis

Traditional therapies for reducing bone loss and fracture risk attributable to osteoporosis include monitoring calcium and vitamin D intake and appropriate physical exercise [13]. A variety of pharmacologic osteoporosis treatments are also routinely prescribed, but their benefits are under question [14]. Oral bisphosphonates are the most common pharmacologic treatment for osteoporosis with more than 30 million actively treated patients worldwide in 2006 alone [15].

1.5 Bisphosphonates

The increase in resorption due to cessation of estrogen production in post-menopausal osteoporosis can be offset by stimulating bone formation or decreasing bone resorption. Bisphosphonates suppress bone resorption [16]. Their chemical structure, which resembles pyrophosphate (Figure 1.4) confers them with a high affinity for exposed hydroxyapatite crystals in active remodeling sites. Once resorbed by osteoclasts, bisphosphonates induce osteoclastic apoptosis which in turn results in reduced osteoclastic activity [17].

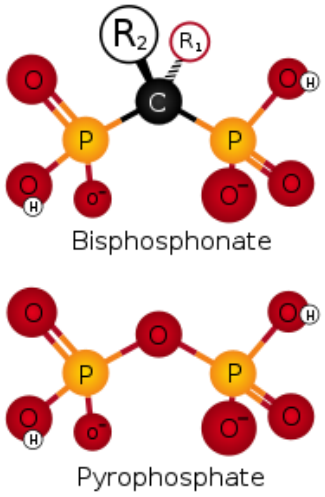

Figure 1.4 Bisphosphonate and Pyrophosphate Structure

Extended periods of reduced osteoclast activity resulting from long term bisphosphonate treatment are known to reduce the rate of bone turnover. Reduced bone turnover allows old and damaged bone to accumulate [17]. This in turn results in impaired load-bearing mechanical competence of such bone, and this in turn renders bone

more susceptible to fracture than bone with normal turnover [18]. Disagreement exists regarding the consequences of increased fracture risk and the benefits of long-term bisphosphonate treatment. Some believe the estimated 1 in 1,000 risk of long-term bisphosphonate related atypical femoral fractures is overshadowed by the overall fracture reducing benefits of the bisphosphonates [19]. Others speculate that 100 osteoporosis-related fractures are prevented for every atypical fracture related to bisphosphonate treatment [20]. Some suggest discontinuing bisphosphonate use if bone mineral density levels are adequate [20].

1.6 Material Property Assessment

There are well established methods for determining the material properties of bone [21]. Macroscopic load to failure testing is the current gold standard for quantifying the bone material properties. Surrogate testing methods with technological advantages have been created and among these is nanoindentation, a spin-off of Atomic Force Microscopy. This method has recently emerged as a useful technique for non-destructive measurement of Young's modulus and hardness of bone with great spatial resolution [21].

The applied force and resulting displacements obtained from nanoindentation testing are recorded from a diamond indenter tip as it is forcibly pressed deeper into a polished flat surface of the material being tested [21]. A portion of the force-displacement unloading slope (Figure 1.5) is used to calculate material modulus by using a model developed by Oliver and Pharr and as quantified in

Equation 1 and Equation 2 [22] [23].

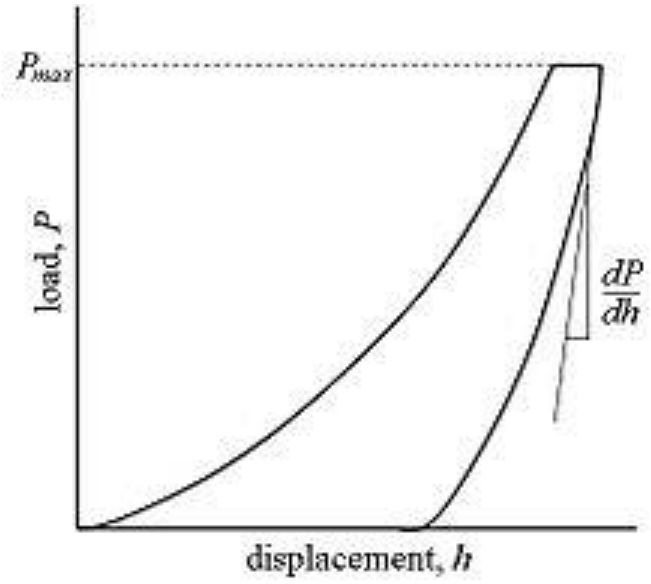

Figure 1.5 Ideal Nanoindentation Load-Displacement Cycle

These calculations assume a flat, polished indenting surface, zero frictional forces, and a material that is linear elastic and incompressible [24] [22]. Calculation of the projected contact area between the probe and indentation surface is based upon the known geometry of the probe and its penetration depth.

Equation 1: Nanoindentation Reduced Modulus

$$E_r = \frac{1}{\beta}\frac{\sqrt{\pi}}{2}\frac{S}{\sqrt{A_p(h_c)}}$$

E_r: Reduced modulus
h_c, β: Geometric constants
$A_p(h_c)$: Projected area of the indentation at the contact depth
S: Stiffness of contact (unloading slope)

Equation 2: Nanoindentation Material Modulus

$$1/E_r = (1-\nu_i^2)/E_i + (1-\nu_s^2)/E_s$$

E_i: Known indentation probe modulus
E_s: Modulus of material
ν_i: Poisson's ratio of probe
ν_s: Poisson's ratio of material

Nanoindentation indent widths can range from 10 to 1000 nanometers which allows a high degree of location specificity. Material properties of bone measured by nanoindentation vary between individuals and specific bones [25] [26]. Variability is also dependent upon indent location and lamellar orientation within the same bone [27] [28] [29].

1.7 Reference Point Indentation

Microindentation techniques load materials in a similar manner to nanoindentation but utilizes larger probe dimensions, greater penetration depths (30-200 microns vs. 10-1000 nanometers), and greater indentation widths (Figure 1.6). Because of the greater size microindentation probes, this technique is influenced by bone porosity, multiple lamellae layers, interfaces between structural units, and microdamage [30].

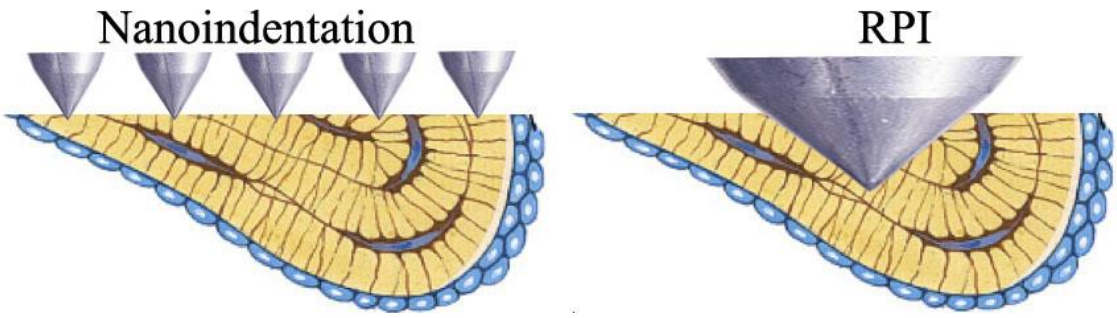

Figure 1.6: Nanoindentation vs RPI Depth in a Trabeculum

RPI instrumentation systems typically include a measurement head unit, measurement stand, and probe assembly (Figure 1.7). The measurement head unit contains a force generator, force sensor, and displacement sensor. The measurement stand enables accurate probe-on-sample positioning by using via an XY translational table to place the indentation probe tip at the desired location. The probe assembly consists of two coaxial components; an indenting test probe that moves coaxially within a reference probe (Figure 1.8). The test probe consists of a 375 micron diameter rod with a 90 degree coned tip having a radius of less than 5 microns [31]. The reference probe consists of a hollow tube (fabricated from a modified hypodermic needle) that coaxially contains the test probe.

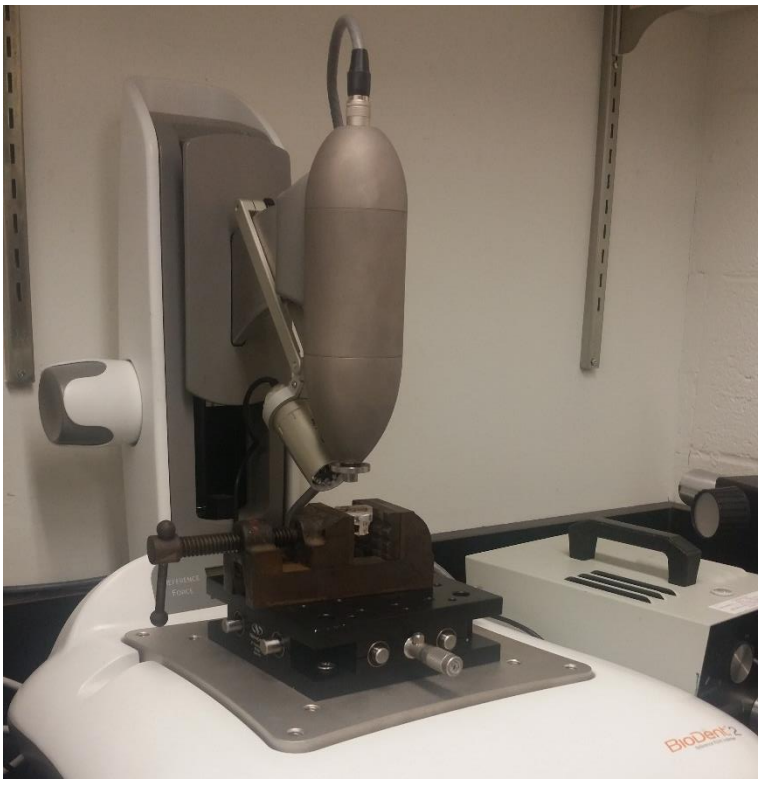

Figure 1.7 Reference Point Indentation Device

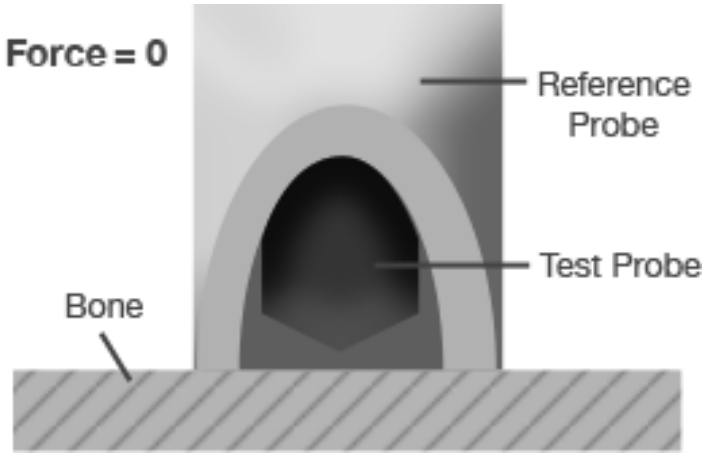

Figure 1.8 Reference Point Indentation Probe Illustration

Reference point indentation begins by first placing the reference probe on the surface of the material to be indented. This locates the site of the test by constraining the test probe from lateral motion across the surface during the indentation process. The test probe repetitively indents the material with a specified number of cyclic indents. Each indentation involves slightly deeper penetration of the probe in the test surface compared

to the previous indent. Transducers in the measurement head record test probe displacement and indentation force throughout this process as the tip of the probe moves within and relative to the surface of the material being indented.

Based upon this set of repetitive indentations and continuous measurement of probe force and accompanying displacement, the test system calculates nine material property relevant parameters based on the time dependent force versus indentation probe displacement. These nine material property relevant parameters are:

1. First cycle indentation distance (ID1st).
2. Total indentation distance (TID)
3. Indentation distance increase (IDI)
4. First cycle creep indentation distance (CID1st)
5. Average creep indentation distance (AvgCID)
6. Average loading slope (AvgLS)
7. Average unloading slope (AvgUS)
8. First cycle unloading slope (US1st)
9. Energy dissipation (ED)

1.7.1 Indentation Depth Parameters (Parameters 1-5)

Five of these parameters (ID1st, TID, IDI, CID1st, and AvgCID) are obtained from test probe force and displacement data (Figure 1.9).

Table 1.1 RPI Parameters

Parameter	How Derived	How Calculated	Relevance	References
ID1st	Probe displacement	After first indentation cycle	Reflects material hardness	[35] [36]
TID	Probe displacement	After last indentation cycle	resist crack initiation and propagation	[32] [33]
IDI	Probe displacement	Difference between first and last indentation cycle	Strength and toughness	[30] [33] [34] [35] [36] [37]
CID1st	Probe displacement	During constant load	Toughness	[38]
AvgCID	Probe displacement	During constant load	Toughness	[38]
AvgLS	Ratio of probe displacement and force	During loading	resistance to plastic deformation	[36]
AvgUS	Ratio of probe displacement and force	During unloading	Strength and toughness	[35]
US1st	Ratio of probe displacement and force	During unloading	Strength and toughness	[35]
ED	Integration of force-displacement curve	Over the entire loading cycle	Toughness	[38]

ID1st is a measure of test probe penetration depth after the first indentation cycle and has been associated with material hardness [35] [36]. TID is the total displacement of the probe into the substrate after all loading cycles and is related to bone's ability to resist crack initiation and propagation [32] [33]. Changes in TID have been associated with changes in: rat vertebrae compressive strength and toughness as well as yield stress

and strength in three-point bending of human femora [35] [33]. IDI is the difference between the initial and final cycle indentation depths. Changes in IDI have been associated with changes in: a) strength and toughness in three point bending of rat femurs, canine ribs, and human femora, and b) strength and toughness in axial compression of rat vertebrae [30] [33] [34] [35] [36] [37].

Reference point indentation also quantifies two material creep-relevant parameters (CID1st and AvgCID) by recording probe displacement while a constant force is maintained on the probe (Figure 1.9). CID1st is the probe displacement during the first cycle of constant load. AvgCID is the average of probe displacement of all constant load cycles. Changes in these creep parameters have been inversely associated with material toughness [38].

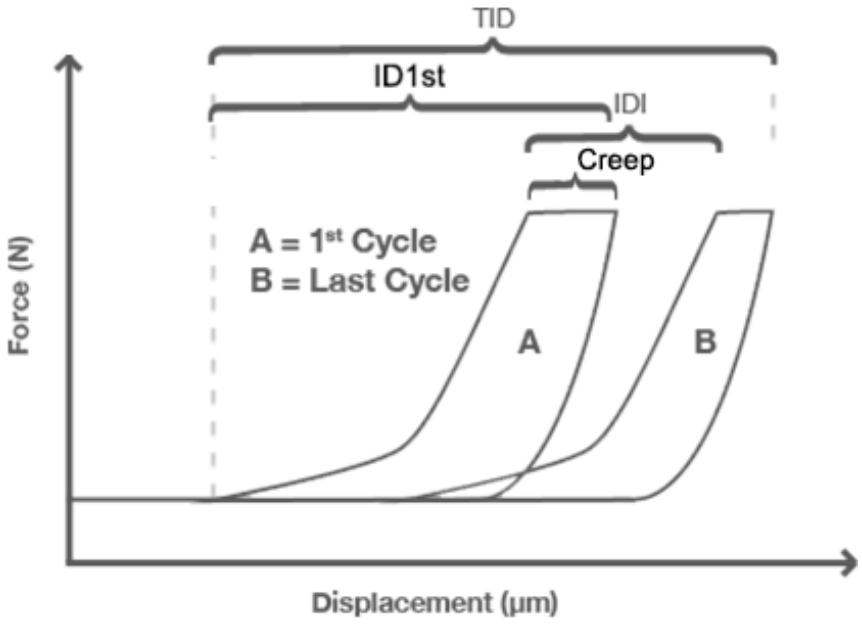

Figure 1.9 Indentation Depth Measurements

1.7.2 Loading/Unloading Slope Parameters (Parameters 6-8)

Three parameters (AvgLS, AvgUS, and US1st) consider the force-displacement slope during loading and unloading of the indentation probe force (Figure 1.10). AvgUS considers the ratio of material strain to test probe force during all indentation cycle while indentation force is decreasing. AvgUS has been associated with strength and toughness as measured by dynamic compression testing [35]. US1st considers the ratio of material

strain to test probe force during the first indentation cycle. Although all of these unloading slope measurements are not a direct measurement of the sample's Young's modulus, they are an indication of Young's modulus [35]. The average unloading slope parameter is able to detect differences between longitudinal and transverse indentations of cortical bone. [36]. AvgLS is similar to average unloading slope but considers the time periods when the test probe force is increasing. It is related to bone's resistance to plastic deformation [36]. AvgLS, AvgUS, and US1st values are calculated (Equations 3-5) using values from the force-displacement graph (Figure 1.10).

Equation 3: AvgLS Calculation

$$\frac{\sum xy - \frac{(\sum x)(\sum y)}{n}}{\sum x^2 - \frac{(\sum x)^2}{n}}, \text{ from (T(N) to P(N))/N.}$$

Equation 4: AvgUS Calculation

$$\frac{\sum xy - \frac{(\sum x)(\sum y)}{n}}{\sum x^2 - \frac{(\sum x)^2}{n}}, \text{ from (R(N) to L(N))/N.}$$

Equation 5: US1st Calculation

$$\frac{\sum xy - \frac{(\sum x)(\sum y)}{n}}{\sum x^2 - \frac{(\sum x)^2}{n}}, \text{ from R(1) to L(1).}$$

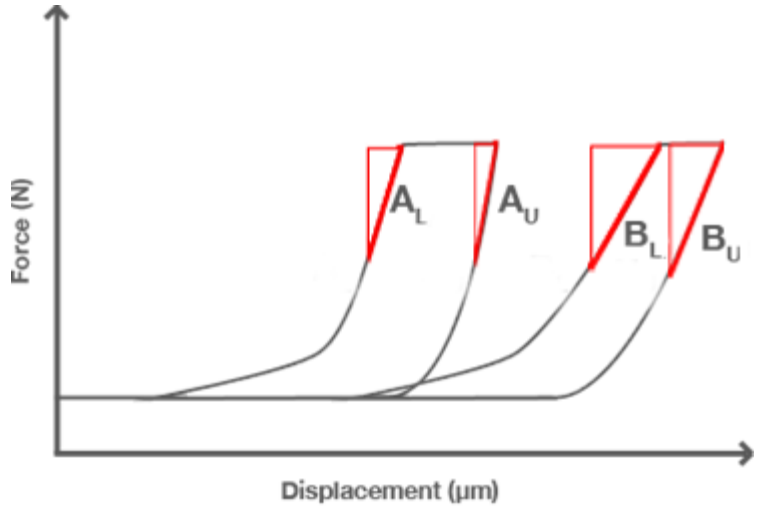

Figure 1.10 Loading and Unloading Slope of Example Materials A and B

1.7.3 Energy Dissipation Parameter (Parameter 9)

Unrecoverable material deformation after indentation is reflected by the energy dissipation (ED) parameter. This parameter is defined by the area bounded by the load and unload curve of the force-displacement relationship (Figure 1.10). This parameter is related to material toughness [33].

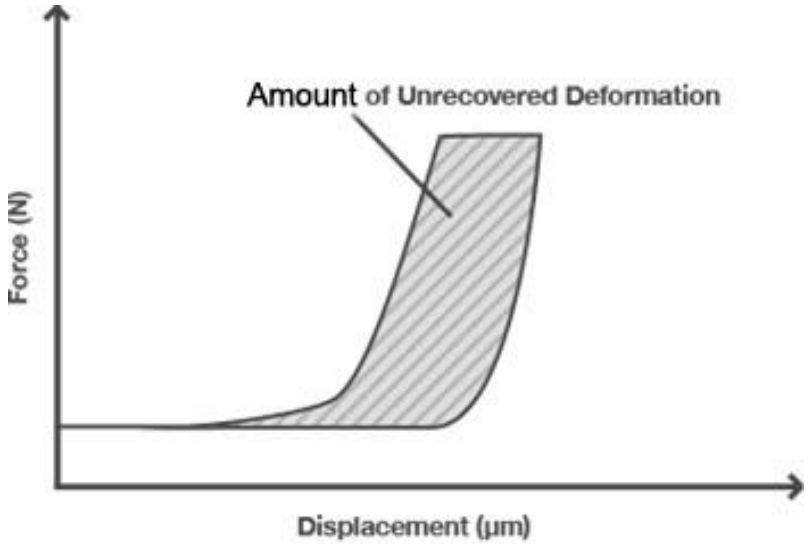

Figure 1.11 Reference Point Indentation Dissipated Energy

1.8 RPI Testing of Bisphosphonate Treated Cortical Bone

Several studies have investigated the effects of bisphosphonate treatment and the resulting changes in cortical bone RPI parameters. Arefa et al. treated beagles with raloxifene for 6 months to measure changes in their bone material properties [34]. RPI testing of the anterior tibial mid shaft surfaces of these beagles was performed using 12 beagles while another 12 were controls that received oral saline only. IDI and ED were approximately 15% less in the treated beagles compared to the control beagles [34]. A related study by Gallant et al. found that healthy beagles treated with bisphosphonates for three years resulted in an approximate 17% increase in cortical rib IDI compared to untreated control beagles [35]. The observed differences in IDI parameters between these two studies may be due to the difference (6 months compared to 3 years) in treatment duration.

Human anterior mid-tibial cortical surfaces were indented by Güerri-Fernández et al. using an early prototype reference point indentation system to investigate differences between patients with: a) atypical femoral fractures treated with bisphosphonates (AFF), b) typical osteoporotic fractures and no BP treatment, c) no fractures with long-term (5 to 12 years) bisphosphonate use, and d) no fractures and no treatment [30]. TID and IDI in patients with atypical femoral fractures treated with bisphosphonates were approximately 25% greater compared to osteoporotic patients with no fractures and no treatment [30].

1.9 RPI and Trabecular Bone

All previous studies that applied microindentation test methods to osseous tissue examined cortical bone exclusively. Application of RPI to trabecular bone is technically challenging due to: limited available surface area of trabeculae relative to probe size, depth of indentation relative to trabeculae depth, and accuracy/precision of indentation probe tip placement on trabeculae. If RPI can be used to quantify the indentation relevant material parameters of trabecular human bone, then additional studies must be conducted to determine accuracy and precision within trabeculae and subjects, as well as intra and inter observer variability.

1.10 Objectives

The objectives of this study were to: 1) determine if RPI use for trabecular bone is feasible and if so, to then determine an optimized test method for using RPI on trabecular bone, and 2) use this optimized method for quantifying the RPI parameters of human trabecular bone treated with BPs for varying durations.

2 Microindentation Testing of Human Trabecular Bone

2.1 Objective

The previously noted challenges attending application of RPI to trabecular bone formed the basis for the first portion of the present research effort. Use of RPI in trabecular bone must be proven feasible by determining whether accurate and precise probe placement and RPI measurements can be made in this bone compartment.

2.2 Theoretical Indentation Depth and Separation Determination

2.2.1 Strain Field Propagation

The purpose of the finite element model was twofold; to determine if the strain and stress field produced by an indentation depth of 50 microns could be confined to the dimensions of a trabeculum and to determine the minimum separation between indents without strain field interference. The volume of trabecular bone permanently altered by an indentation using RPI is primarily influenced by the probe size and indentation force. While probe size is fixed, increasing probe indentation force increases the indentation depth. Increasing the indentation depth reduces measurement uncertainty due to the device's linear transducer measurement resolution which rounds to the nearest micron. Therefore, a measured 50 micron indentation depth could actually be between 49.5 microns and $50.4\overline{9}$ microns. Since all trabecular bone samples are embedded in PMMA, an indent larger than the trabecular width or depth would deform the PMMA mounting material and result in testing material that was not 100% trabecular bone. The deformation size produced by an indentation can be estimated using finite element modeling to determine an optimal indentation force.

2.2.2 Indentation Separation

Minimizing indent separation distance increases the total number of indents possible in a sample of limited trabecular surface area. Indent separation distance must be large enough to avoid strain field interaction between adjacent indents. Identification of this minimal indentation separation distance can be estimated using finite element analysis.

2.2.3 Finite element method

Deformation of a simple structure with known material properties caused by an applied force can be calculated using standard deformable solid body mechanics. Finite element analysis allows larger, more complex structures to be analyzed in the same manner by conjoining a finite number of simple shapes together. Each simple shape, deemed an element, can be represented by a line, triangle, quadrilateral, or any shape solvable with partial differential equations. The deformable solid calculations for these numerous elements can be solved simultaneously to determine theoretical stress and strain within a complex structure given assumed boundary conditions, deformations, and forces acting upon the structure. This method of using numerous smaller elements to analyze a complex deformable solid structure was originally developed by Ray W. Clough in 1960 and is known as finite element analysis [39].

2.2.4 Model Geometry, Constraints, and Properties

The finite element model for trabecular bone indentation was based upon a single body having linear elastic geometry. The indentation was represented by a force distribution. The trabeculum to be indented was assumed to be a simple semi-cylinder with the center of indentation placed along the cylindrical axis. Three planes of symmetry were used in this model (Figure 2.1). The first plane of symmetry was normal to the cylindrical axis and placed at varying distances from the center point of indentation. The second plane of symmetry was normal to the cylindrical axis and passed through the center point of indentation. The separation between the first and second symmetry planes represented half of the theoretical separation distance between indents. The third plane of symmetry was parallel to the cylindrical axis and perpendicular to the indentation surface. This plane of symmetry transforms the semi-cylinder into a quarter-

cylinder. The planes of symmetry are constrained in both X and Z directions. The remaining circumferential surface of the cylinder, representing the boundary with PMMA, was assumed to be a fixed support. The orientations of the three planes are shown (Figure 2.1). The elastic modulus and Poisson's ratio values used to represent trabecular bone were assumed to be 10 GPa and 0.3 [40]. Although bone is a viscoelastic material, for purposes of this model it was assumed that bone was linearly elastic, isotropic, and homogeneously mineralized.

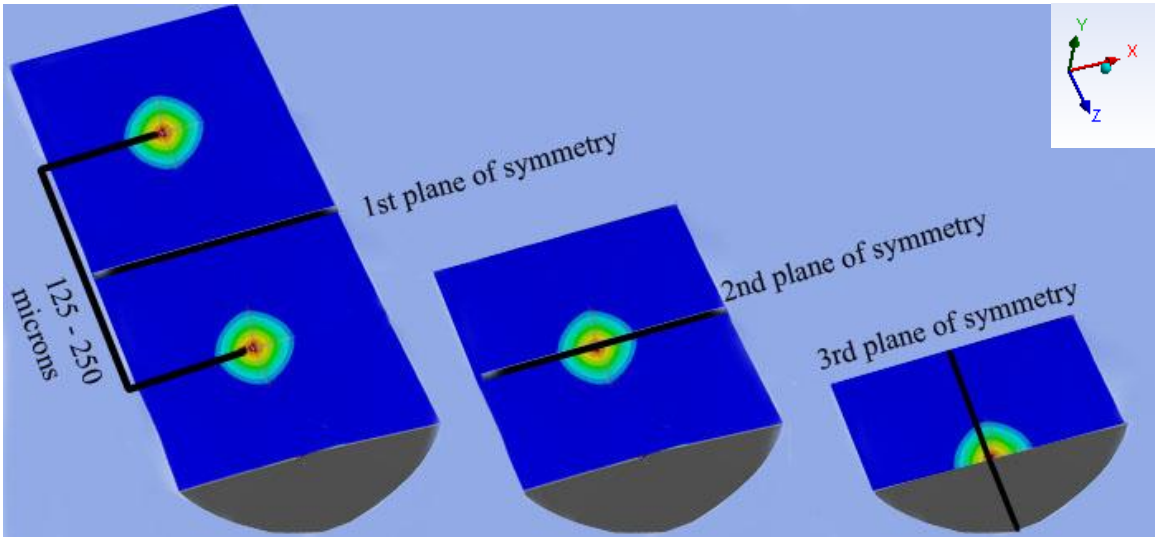

Figure 2.1 ANSYS Model Symmetry Planes

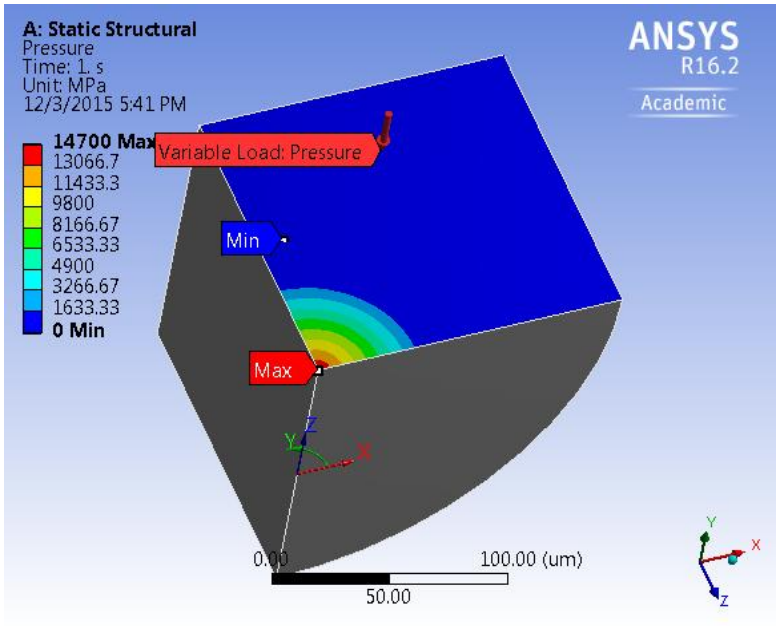

Figure 2.2 ANSYS Variable Load Pressure Indentation Model

2.2.5 Material Properties and Indentation Force Modeling

The indentation force used in the model was represented by a triangularly shaped non-uniform pressure distribution normal to the indentation surface and axisymmetric to the center point of indentation (Figure 2.2). The length of the non-uniform pressure was 50 microns based on a 90 degree indentation probe tip angle and a target indentation depth of 50 microns. Therefore, the pressure at the edge of the resulting 100 micron diameter indent was zero and the pressure at the center of the indent was determined by trial and error until the largest deformation in the body was approximately 50 microns.

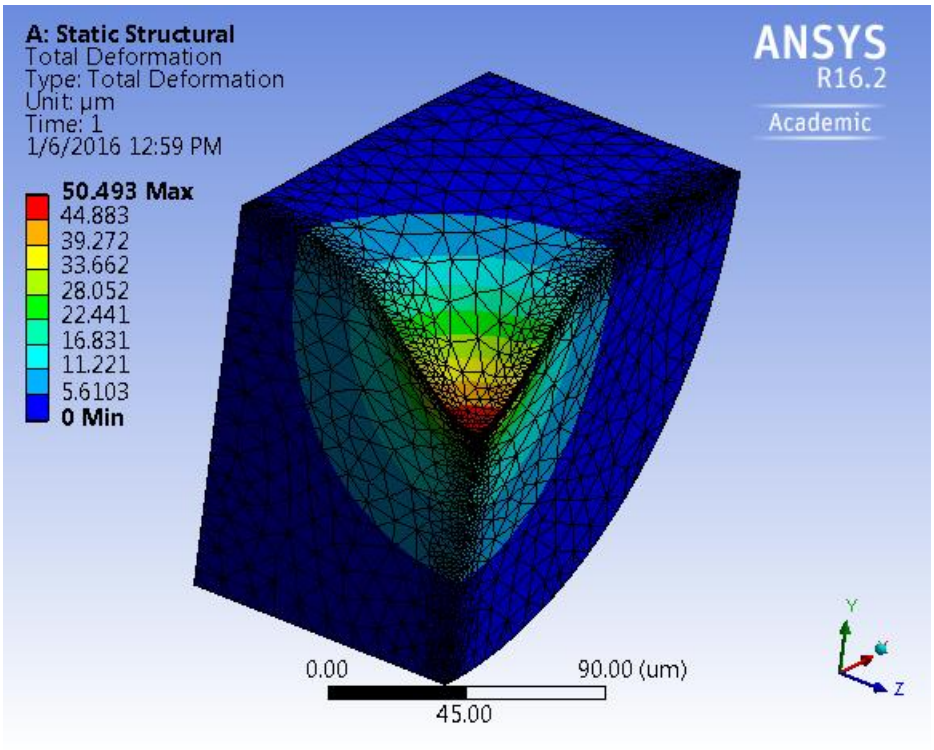

Figure 2.3 Strain Plot of 200 micron Indent Separation

2.2.6 Theoretical Results

The FEA model of probe indentation into bone was solved using 11 varying center-to center probe indentation distances ranging from 250 to 125 microns. Total deformation of the structure resulting from the controlled pressure distribution was calculated. The largest deformation determined the indentation depth and this value was plotted versus the separation between indents (Figure 2.4). This plot shows that indentation depth increases exponentially when center-to-center indentation distances decrease and become less than 175 microns.

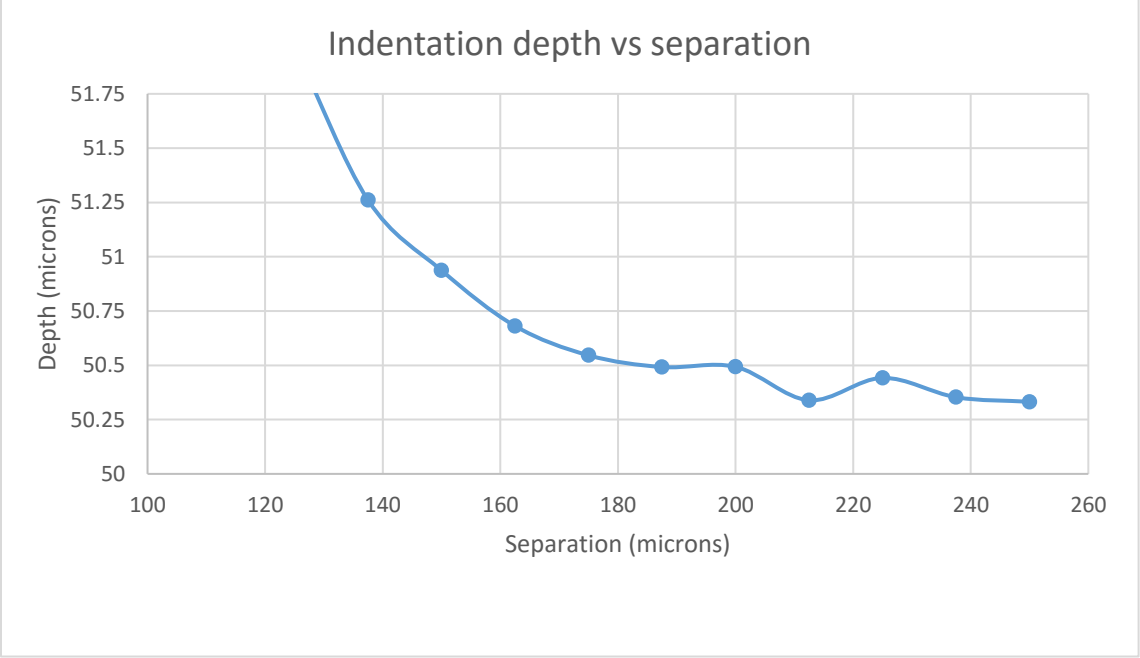

Figure 2.4 Indentation Depth versus Indent Separation

2.2.7 Theoretical Discussion

The strain and stress fields propagated in the trabeculum without interacting with the lower or edge boundary conditions for the assumed trabeculae size of 280 microns. Figure 2.3 shows an indentation depth of 50 microns will not interact with PMMA considering the dimensions of this trabecular bone model.

The device's transducer measures to the nearest micron. Therefore if strain field interference between two adjacent indents results in a depth variation of less than 1 micron the device will not detect it. This occurs if the center-to-center indentation distances are greater than 175 microns. The finite element model used assumed that a 4 Newton indentation force was used to produce the indentations. Four N of indentation force in preliminary experimental testing using actual human trabecular bone samples was the maximum observed indentation force which showed minimal risk for penetrating a trabeculum.

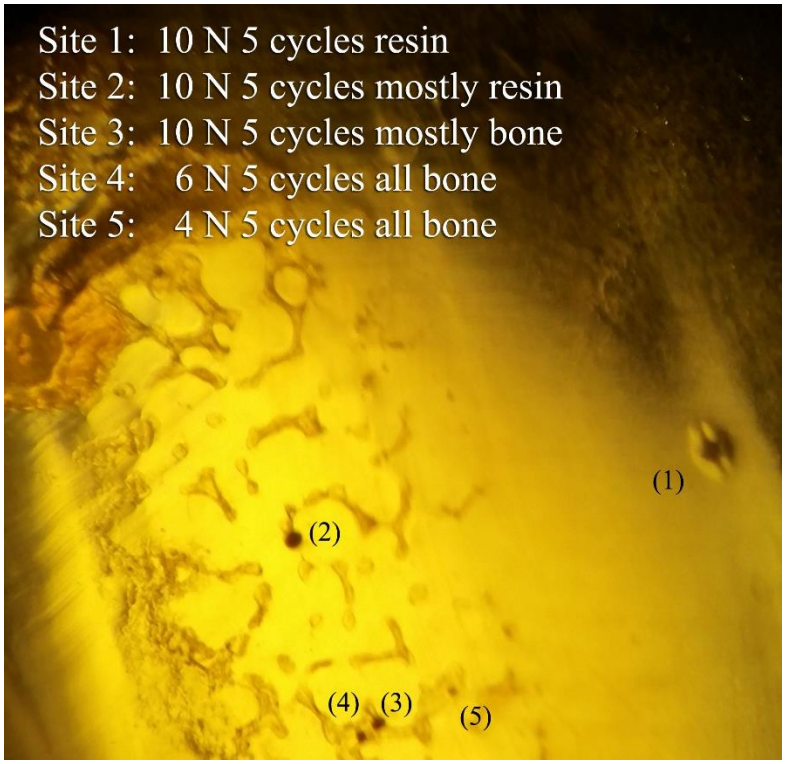

Figure 2.5 Indentation Sizes of Different Protocols

The limitations of the FEA model used were attributable to assumptions made regarding material properties, trabecular shape and size, and indentation force. Although the shape of the modelled trabeculum does not affect propagation of the strain field caused by the indentation, provided that the strain field does not extend to the surface of the trabeculum. A vertical axisymmetric pressure distribution does consider force vectors and shear forces associated with indentation. The shape and size of the indent and resulting strain field are comparable to the experimental microindentation when only considering the effects of indentation separation and depth. These results were verified by the low coefficient of variation seen between adjacent indents separated by 200 microns in the following section (2.3).

2.3 Experimental Indentation Protocol and Sample Size Determination

2.3.1 Maximizing Sample Size

Results of the FEA model show that a force of 4 N and a separation of 175 microns were optimal for reference point indentation of trabecular human bone. Next, the sources of experimental variance needed to be identified and the contributions from each estimated so that an optimal RPI testing protocol could be developed. This protocol needed to be as sensitive as possible to allow the relationship between BP treatment duration and one or more RPI parameters to be elucidated, if such relationships do in fact exist. Specific testing parameters targeted for optimization included the: number of indents per sample, the number of trabeculae tested per sample, and the number of samples. A balance needed to be achieved for the total number of indents per sample so that random error could be minimized while maximizing the number of samples with adequate trabecular surface area for testing. The estimated random error of each possible protocol can be used to determine the optimal indent quantity per location within a sample. The objective of this experimental portion of the study was to determine which protocol had the least variance.

2.3.2 Methods

Two groups (pre and post-menopausal) of four homogenous ex vivo trabecular bone samples from otherwise identical pre and post-menopausal women were obtained. Samples consisted of low turnover bone from osteoporotic Caucasian female patients

with no history of: bisphosphonate treatment, hormone therapy, cancer, recent smoking, steroid use, chronic kidney disease, or diabetes. 55 bone samples matching these criteria were obtained. These samples were prepared for RPI testing and then indented three times on each of 3 trabeculum per sample for a total of nine indentations per bone sample.

The results were used to calculate the observed variance between: a) bone samples (σ_b^2), b) trabeculae within a bone sample (σ_t^2), and c) indents within a trabeculum (σ_i^2) for each RPI parameter by analyzing the variance within each level of the hierarchical design. The observed variances were used to estimate the variance for other candidate indentation protocols using Equation 6.

Equation 6: Estimated Coefficient of Variation for Candidate Protocols

$$CV_X = \frac{\sigma_B}{N_B\overline{X}} + \frac{\sigma_T}{N_B N_T \overline{X}} + \frac{\sigma_I}{N_B N_T N_I \overline{X}} * 100$$

Where

$\overline{X}$ = Output parameter mean

σ = Observed variance between indents (σ_I), trabeculae(σ_T), and samples (σ_B)

N = Number of indents (N_I), trabeculae (N_T), and biopsies (N_B) considered

Coefficients of variation for each RPI parameter were averaged so that each protocol and sample size could be represented by a single coefficient of variance. There were a total of 14 bone samples treated 10 or more years with bisphosphonates constituted the fewest number of samples. This important subset of the available samples formed the basis for determining the experiment that maximized the information from these samples and minimized the variance in observed RPI parameters. These samples were collected and visually examined for available cross sectional trabecular area. Each exposed trabeculum on each of these 14 samples was estimated for the number of times it could be indented assuming 200 microns of indentation separation and 4 N of indentation force. Quantification of the area in each sample, in units of indentation quantity, allows a maximum number of available samples to be identified given a specific indentation protocol. The number of trabeculae in each sample that can be indented given a specific number of indents is shown (Table 2.1).

2.3.3 Experimental Results

All candidate indentation protocols, based upon indent allocation and sample size, were represented by a single coefficient of variation for each parameter. The calculated coefficient of variances for 5 to 14 bone samples, 1 to 5 trabeculae per sample, and 1 to 4 indents per trabeculum were plotted MATLAB. Figure 2.6 shows the coefficient of variance for the total indentation depth parameter for each of the combinations. Each possible candidate protocol and its corresponding average coefficient of variation was compiled and ranked by variance in

Table 2.2.

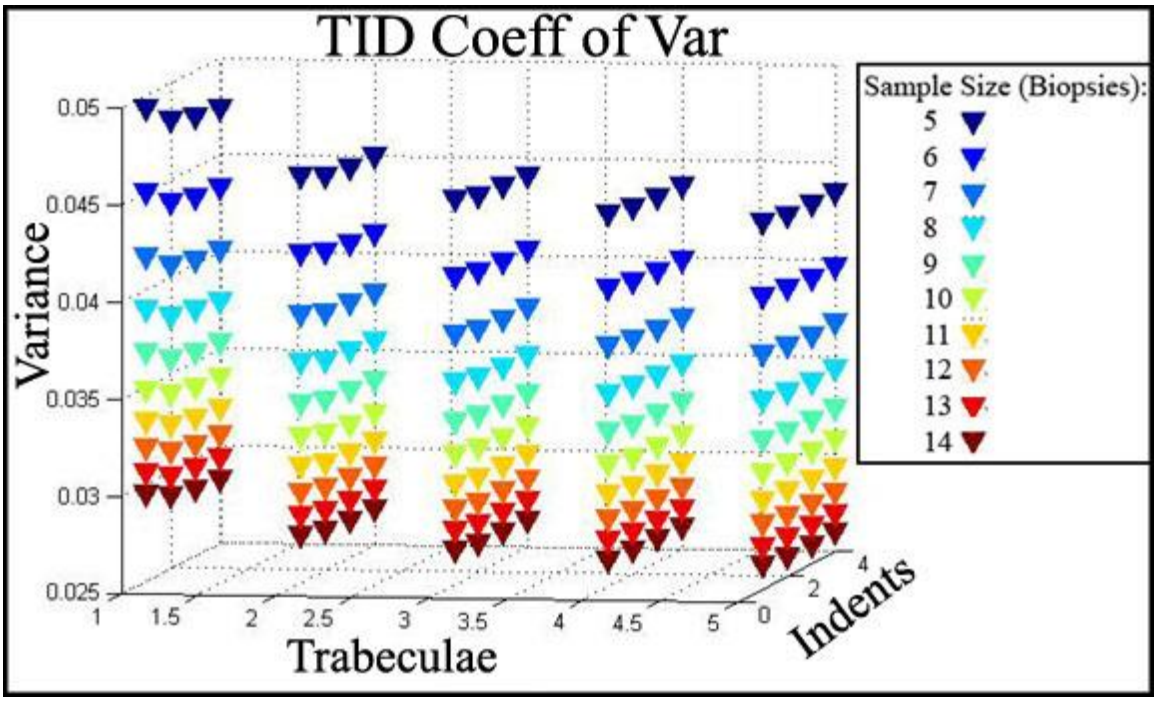

Figure 2.6 Total Indentation Depth Predicted Coefficient of Variation

Table 2.1 Possible Indentations in 10+ Year Treated Samples

		# of Indents per Trab			
	Bone Sample ID Number	**4**	**3**	**2**	**1**
# of Trab	B05411	0	1	2	3
	B07507	0	2	3	4
	B10710	2	2	5	5
	B03911	0	2	3	3
	B05610	1	2	6	6
	B02912	0	1	2	2
	B04208	0	1	3	3
	B09111	0	2	5	6
	B04110	1	3	5	5
	B05310	1	3	7	7
	B06110	1	2	4	4
	B03109	2	4	6	6
	B04612	0	0	1	1
	B07010	1	1	4	4

Table 2.2 Possible Protocols, Maximum Sample Size, and Coefficient of Variation

Possible Protocol and Resulting Variation			
Trab	**Indents**	**Samples**	**Avg C of V**
2	2	13	0.0317
2	1	13	0.0326
3	2	11	0.0332
1	2	14	0.0336
1	3	13	0.0343
1	1	14	0.0351
4	1	9	0.0366
2	3	9	0.0377
4	2	8	0.0382
5	2	6	0.0436
5	1	6	0.0442
1	4	7	0.0464

2.3.4 Experimental Discussion

The largest contributor to the observed variance was the number of indented bone samples. The second largest contributor to the observed variance was the number of trabeculae indented followed last by the number of indentations on each trabeculum. The degree of contribution for each protocol variable is evident in the three-dimensional plot in Figure 2.6. Increasing the number of indented samples is the most efficient means of decreasing random error.

Variance between samples outweighs variance within the sample because the proximity of indents in a single sample. Indents within a sample are no more than a few centimeters apart. Indents within a trabeculum are measured to a consistent 200 microns apart. Although material properties of bone have been shown to vary in different locations of the same bone [41], they are more likely to vary between patients than within a sample. Bone homogenization due to bisphosphonate treatment may reduce this variance between treated patients [4] [41].

2.4 Conclusion

Reference point indentation using two indents per trabeculae and two trabeculae per bone sample offered the lowest calculated CV and was therefore selected for use based upon the samples available for examining the relationship between bisphosphonate treatment duration and the RPI parameters. Finite element modeling determined minimal indentation separation to be 175 microns to avoid detectable strain field interaction. Indentations depths of 50 microns showed no interaction upon the trabecular boundary with PMMA.

3 RPI of Trabecular Bone with Varying Bisphosphonate Treatment Duration

3.1 Objectives

The objective of this study is to determine if any RPI parameters (refer to the list cited in section 1.7) are related to the duration of bisphosphonate treatment in human trabecular bone by implementing the previously established RPI testing procedure.

3.2 Methods

3.2.1 Study Design

The dependent variable in this cross sectional study was an individual's duration of bisphosphonate treatment in years. The independent variables were the RPI output parameters (section 1.7). The sample size was expected to be approximately 40. Analysis of variance was used to relate each RPI parameter with BP treatment duration. Multiple regression analysis was used to consider the following covariates: age, bone volume per total volume, bone mineral density, hormone therapy, fracture history, exercise, calcium supplement use, and prescription vitamin D use. This study conforms to the Declaration of Helsinki and was approved by the University of Kentucky IRB.

3.2.2 Inclusion Criteria

Bone samples were obtained from anterior iliac crest biopsies taken from osteoporotic post-menopausal Caucasian female patients between 41-87 years of age who had low bone turnover. These bone samples were catalogued in the Kentucky Bone Registry maintained by the University of Kentucky's Division of Nephrology and identified by electronic database.

3.2.3 Exclusion Criteria

Samples excluded from patients with: osteogenesis imperfecta, osteomalacia, any genetic bone disease, hyperparathyroid disease, chronic kidney disease, Paget's disease of bone, a history of drug or alcohol abuse, a history of smoking, SERM use, steroid use, teriparatide treatment, and any medications/disease known to alter bone metabolism.

3.2.4 Procedure

Bone samples in the registry were previously embedded in poly methyl methacrylate (PMMA) for processing and preservation. Embedded bone samples that were enrolled in this study were cut to show trabecular cross sections. Each cross sectioned surface was ground and polished flat and smooth using abrasive silicon carbide papers of decreasing grit size (ending in 1200 grit). A final polish was achieved using a rotating micro cloth wetted with deionized water and suspended diamond particles (0.3-μm grit size and then 0.05-μm grit size). Samples were placed in an ultrasonic water bath for 10 minutes to remove grinding and polishing debris.

Each sample was clamped in a vice with its polished surface oriented horizontally (Figure 3.1). The sample was visually accessed under a Bausch & Lomb Stereozoom 4 stereo microscope. Differentiating areas of PMMA and exposed bone on the surface of each sample was difficult due to the polished surface and lack of color contrast. The distinction could only be made when a directional light source was reflected off the surface to the observer to better reveal surface texture. The smooth, polished PMMA surface appears glossier than texturized bone tissue as shown in Figure 3.2.

Figure 3.1 Trabecular Bone Sample Secured in Vice with V-block Insert

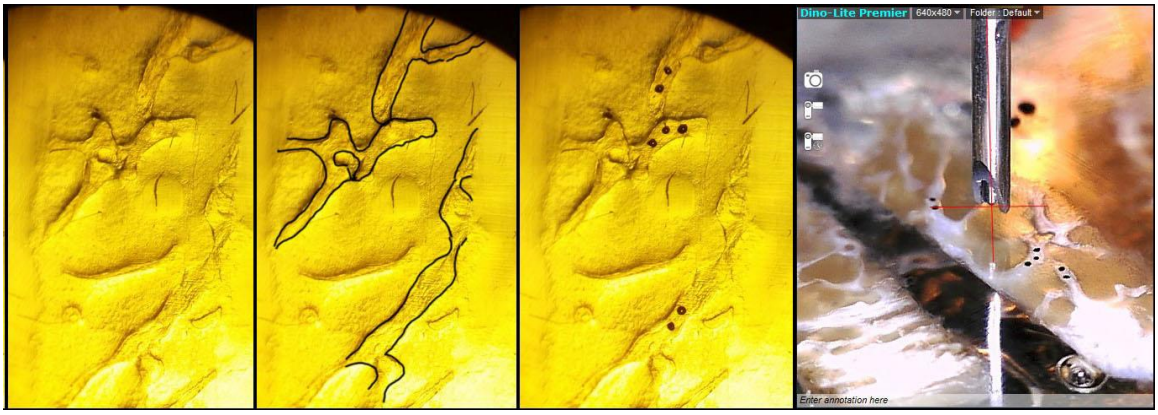

Figure 3.2 Trabeculae Identification and Probe Placement

Placing ink dots on potential indentation sites allowed for more accurate aiming of the probe once the sample was in the machine. While viewed through the stereo microscope (Figure 3.2) ink dots of approximately 80 microns diameter were placed on trabecular areas of sufficient size to accommodate two indentations set 200 microns or more apart. Two trabeculae from all trabeculae identified as having sufficient available test surface area were chosen for indentation at random using a coin flip. The mounted (V-block, Figure 3.1) sample was then placed onto the horizontal test stage of the RPI instrument and rotated so that an imaginary line between two potential indents aligned with the translational table's X or Y axis (Figure 3.3).

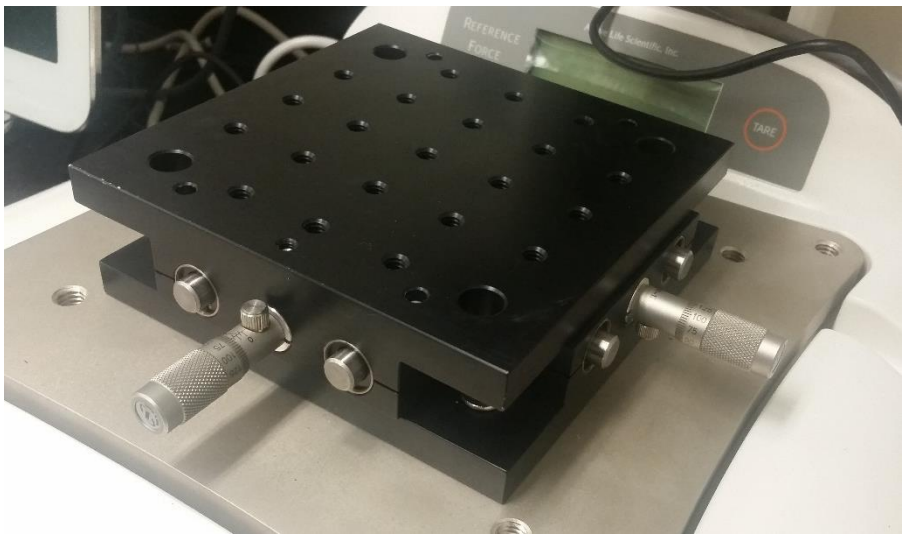

Figure 3.3 X Y Translation Table for Measuring Indent Separation

The RPI head unit was positioned over and lowered onto the sample surface until the RPI device's scale registered a preload of 530-570 grams. A maximum indentation force of 4 N was used in this study. Preloading the sample insured that the reference probe maintained its XY position on the sample surface during indentation. After indentation, the head unit and indentation probe were raised off the sample surface and the sample was moved 200 microns to the next indentation site using a single axis of the XY translational table. The resulting indents are shown in Figure 3.4.

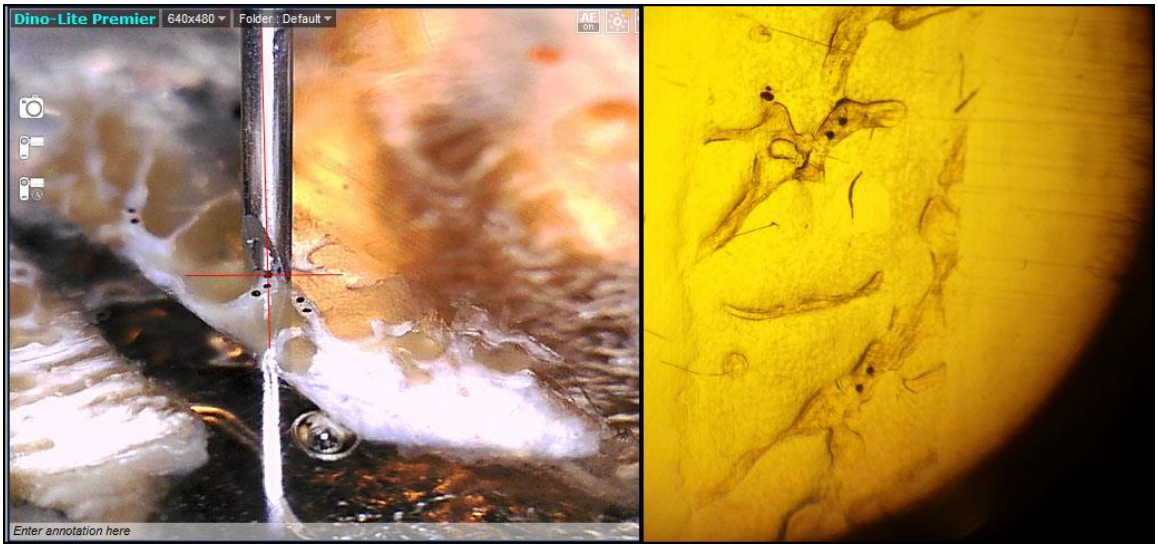

Figure 3.4 Probe Placement and Resulting Indents

After translating the sample 200 microns the head unit was lowered to a preload of 530-570 grams and the second indentation was made. The procedure was repeated to indent the second trabeculum to complete a total of four indents in each sample. Indentation validity was defined by the indentation depth, shape of the force vs. displacement graph, and visual inspection of the indent. Visual PMMA deformation around an indent or a hole in the center of the indented bone tissue is the best indicator of an invalid indent (Figure 3.5 Characteristics of an Invalid Indent Results

Results

Unusually high indentation depths and low loading slopes displayed by the device software (measured values at least 30% different than the average value recorded in each sample) may indicate that an indentation involved both PMMA and bone. This can occur

if an indent is too close to the edge of a trabeculum or if a trabeculum has insufficient depth or width to sustain an indentation. Invalid indents were noted in the software and excluded from data analysis.

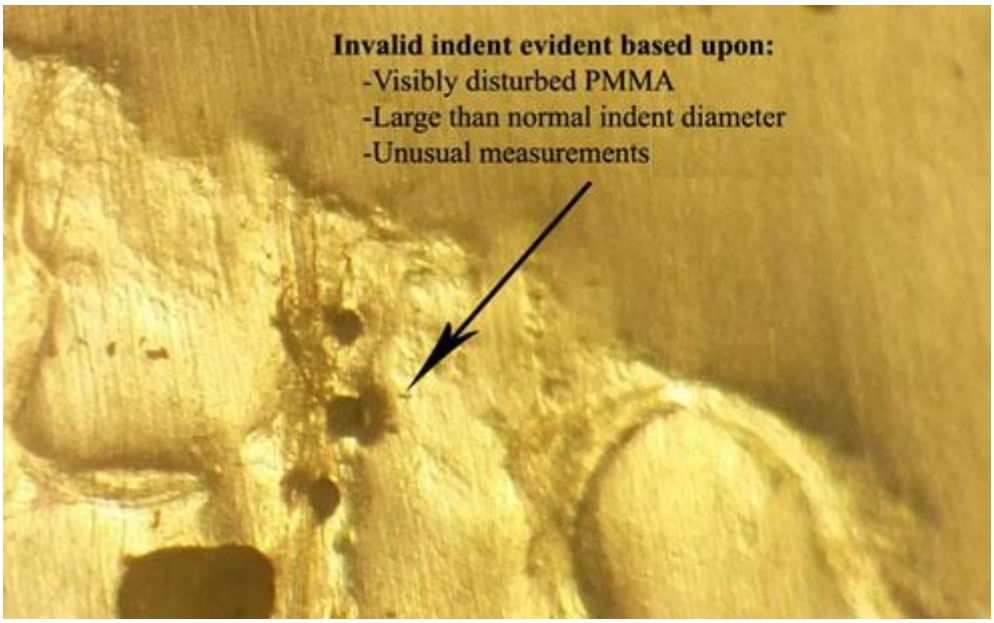

Figure 3.5 Characteristics of an Invalid Indent Results

3.3 Results

Of the 58 samples meeting the inclusion criteria, but not the exclusion criteria, 44 were enrolled in the present study and successfully indented. Samples not indented had inadequate exposed surface area or failed accommodate the selected indentation protocol given the previously discussed validity criteria. Samples from bisphosphonate treated subjects (0.3 to 14 years) and five samples from untreated osteoporotic subjects were indented.

Indentation distance increase (IDI, section 1.7) (p=0.012), first cycle unloading slope (US1st) (p=0.048), and average unloading slope (AvgUS) (p=0.029) were significantly correlated with bisphosphonate treatment duration. When considering the covariates age and calcium supplementation use, indentation distance increase (IDI) (p=0.001), total indentation depth (TID) (p=0.049), energy dissipated (ED) (p=0.042), first cycle unloading slope (US1st) (p=0.028), average unloading slope (AvgUS) (p=0.012), and average loading slope (AvgLS) (p=0.049) significantly correlated with bisphosphonate

treatment duration. These RPI parameters were optimally related to subject age, calcium supplementation use, and bisphosphonate treatment duration using Equation 7.

Equation 7: Multivariate Regression Equation

$$Parameter = \beta_0 + \beta_A(Age) + \beta_C(Calcium) + \beta_D(BP\ Duration)$$

Where,

β_0:	RPI Parameter Intercept
$\beta_A, \beta_C, \beta_D$:	Coefficient for Age, Calcium Use, and Treatment Duration
Age:	Age of Patient in Years
Calcium:	Binary Value for Patient Calcium Supplementation
BP Duration:	BP Treatment Duration in Years

None of the other 9 RPI parameters (CID, CID1st, and ID1st) were related to bisphosphonate treatment duration despite consideration of all listed covariates. The multiple regression equation coefficients for the 6 correlated RPI parameters are shown (Table 3.1). Linear regression plots for each of these 6 equations are provided (Figure 3.6-Figure 3.11).

Table 3.1 Multiple Regression Equation Coefficients

	IDI	TID	ED	US1st	AvgUS	AvgLS
b_0	4.9070	44.092	11.38855	0.29434	0.29172	0.20779
b_A	-0.00979	-0.03811	-0.01809	0.00026	0.00035	0.00021
b_C	-0.45104	-1.23064	-0.81775	0.00764	0.01001	0.00550
b_D	0.04678	0.10300	0.10206	-0.00136	-0.00158	-0.00080

Table 3.2: p Values for Regression Equation Coefficients

	IDI	TID	ED	US1st	AvgUS	AvgLS
b_A	NS	NS	NS	NS	NS	NS
b_C	0.0017	0.0188	NS	NS	NS	NS
b_D	0.0013	0.0490	0.0423	0.0284	0.0118	0.0485

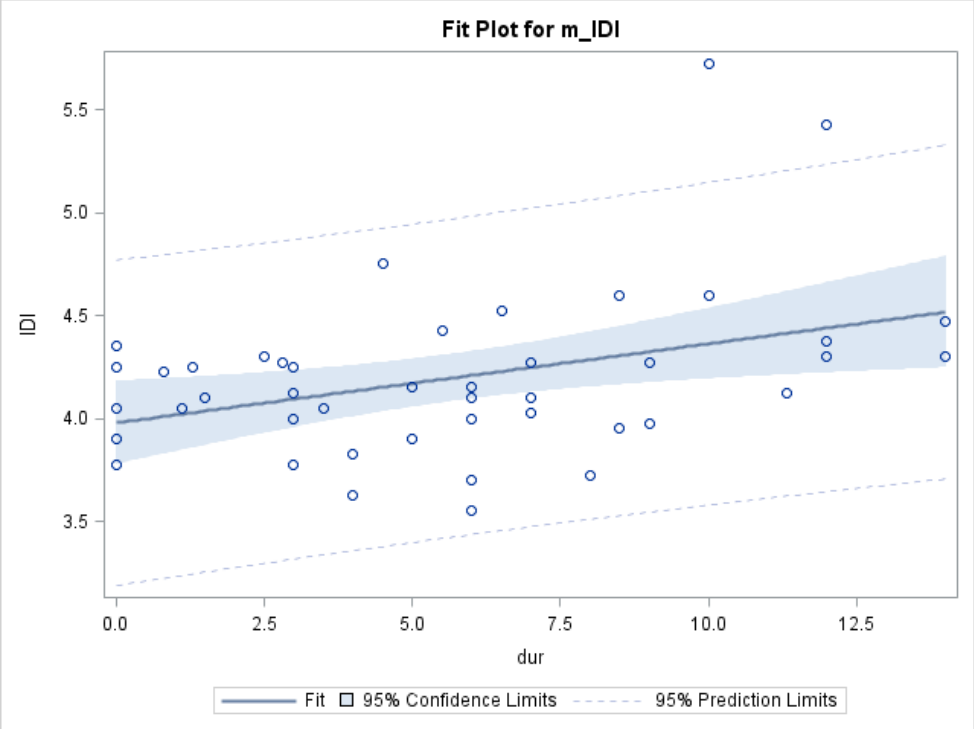

Figure 3.6 Indentation Distance Increase (IDI, µm) vs Bisphosphonate Treatment Duration (dur, years) (p=0.0115) (R^2=0.34)

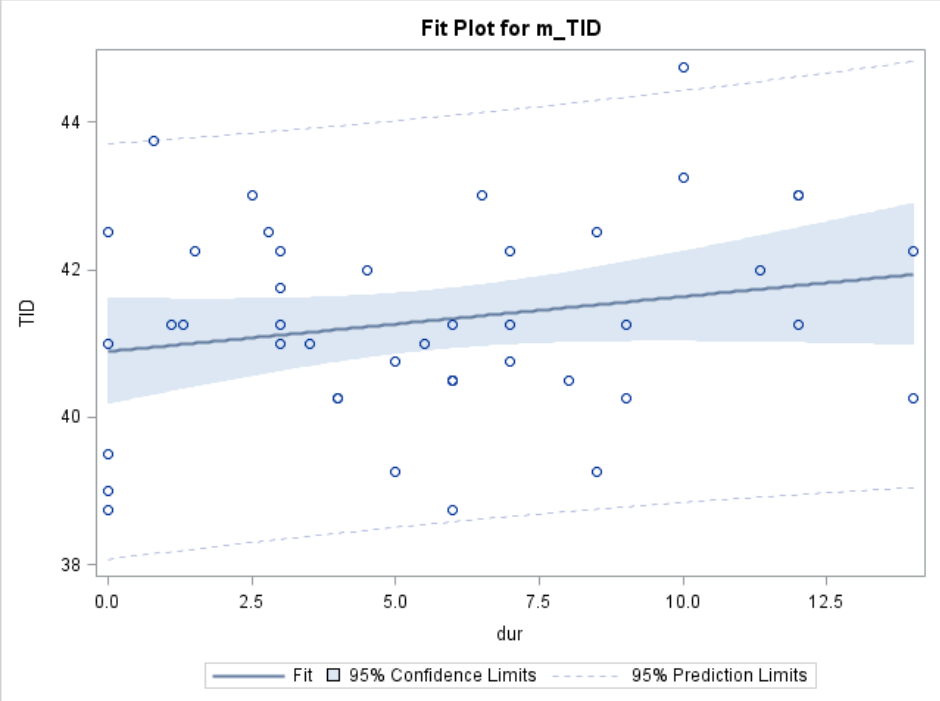

Figure 3.7 Total Indentation Depth (TID, µm) vs Bisphosphonate Treatment Duration (dur, years) (NS) ($R^{2=}$0.19)

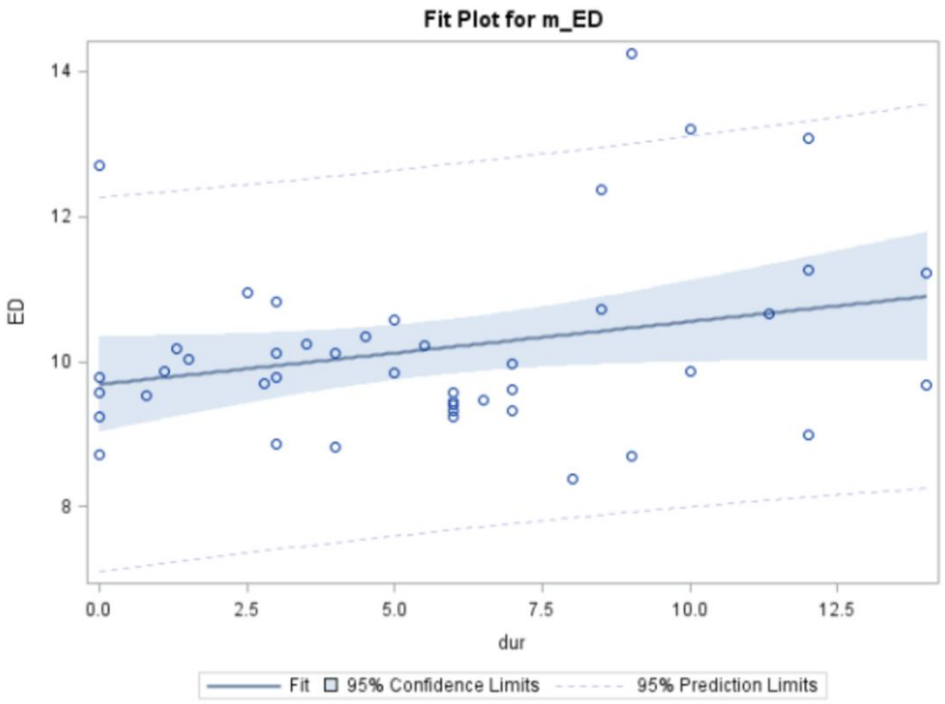

Figure 3.8 Energy Dissipated (ED) vs Bisphosphonate Treatment Duration (dur, years) (NS) (R^2=0.14)

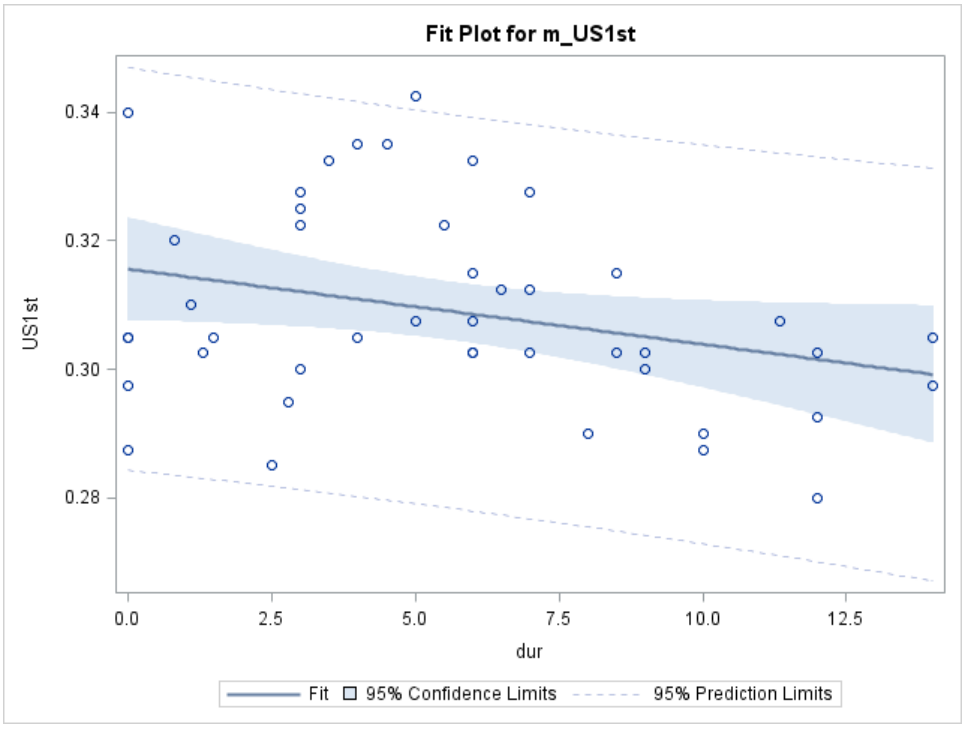

Figure 3.9 1st Cycle Unloading Slope (US1st) vs Bisphosphonate Treatment Duration (dur, years) (p=0.0481) ($R^{2=}$0.13)

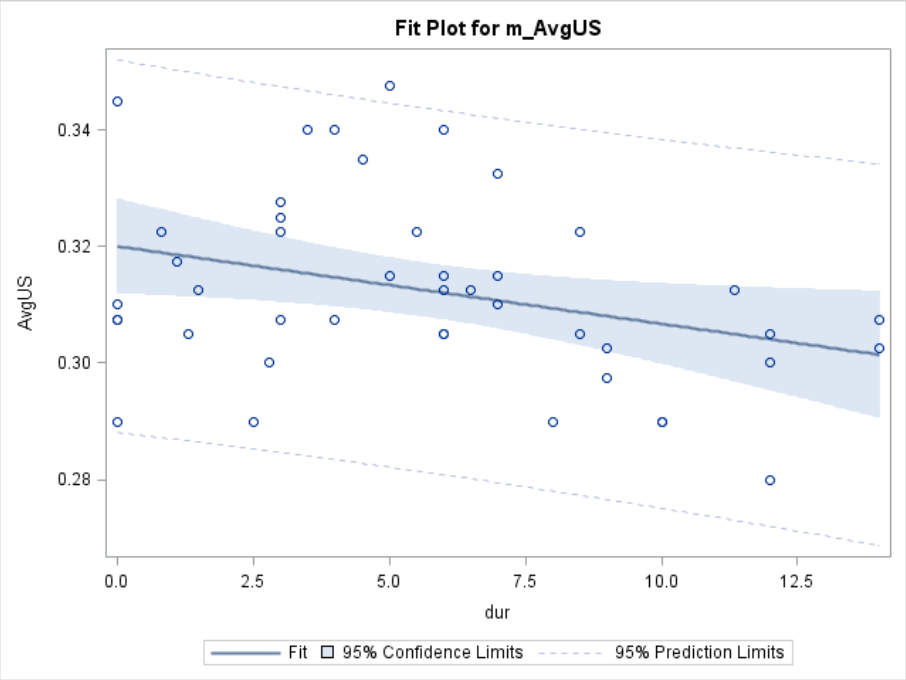

Figure 3.10 Average Unloading Slope (AvgUS) vs Bisphosphonate Treatment Duration (dur, years) (p=0.0286) ($R^{2=}$0.18)

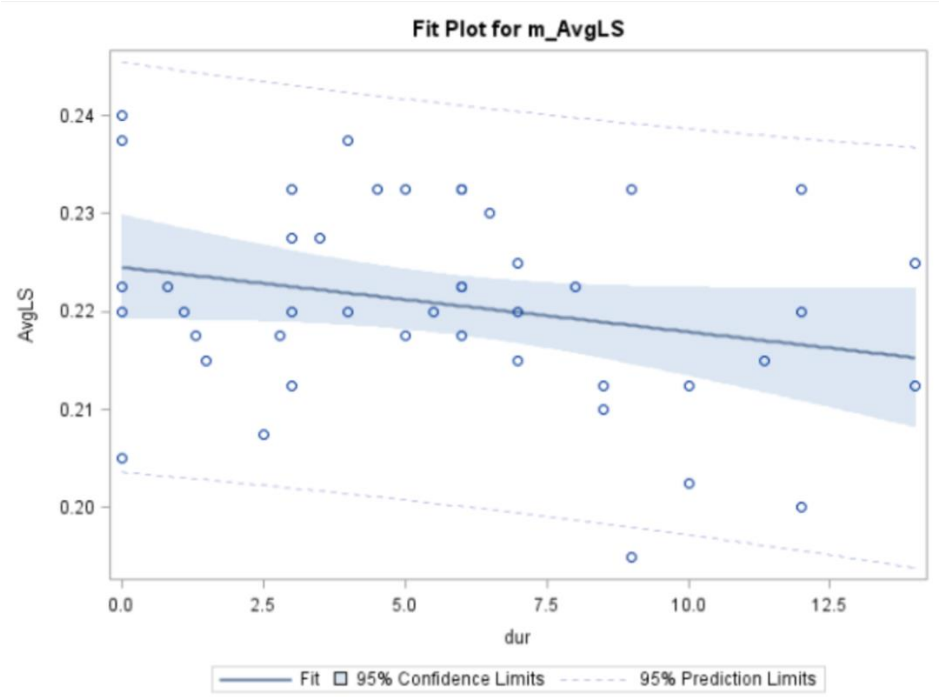

Figure 3.11 Average Loading Slope (AvgLS) vs Bisphosphonate Treatment Duration (dur, years) (NS) (R^2=0.12)

3.3.1 Calcium Supplement Usage

Subjects who did not report using calcium supplementation were found to follow a significantly higher regression slope than those not taking a supplement. This difference between regression slopes was found by testing the interactive relationship between variables of calcium supplementation and treatment duration within the multivariate regression models for TID and IDI. Figure 3.12 and Figure 3.13 show the differences in regression slope with (35 patients) and without (7 patients) calcium supplementation for TID and IDI.

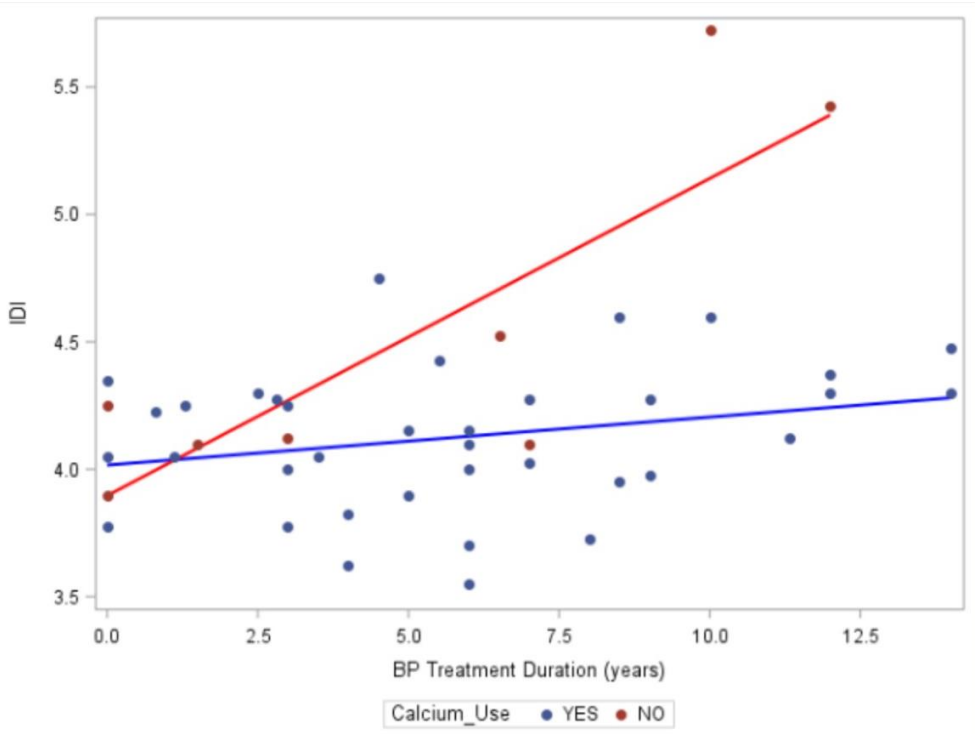

Figure 3.12 IDI vs Treatment Duration Considering Calcium Usage

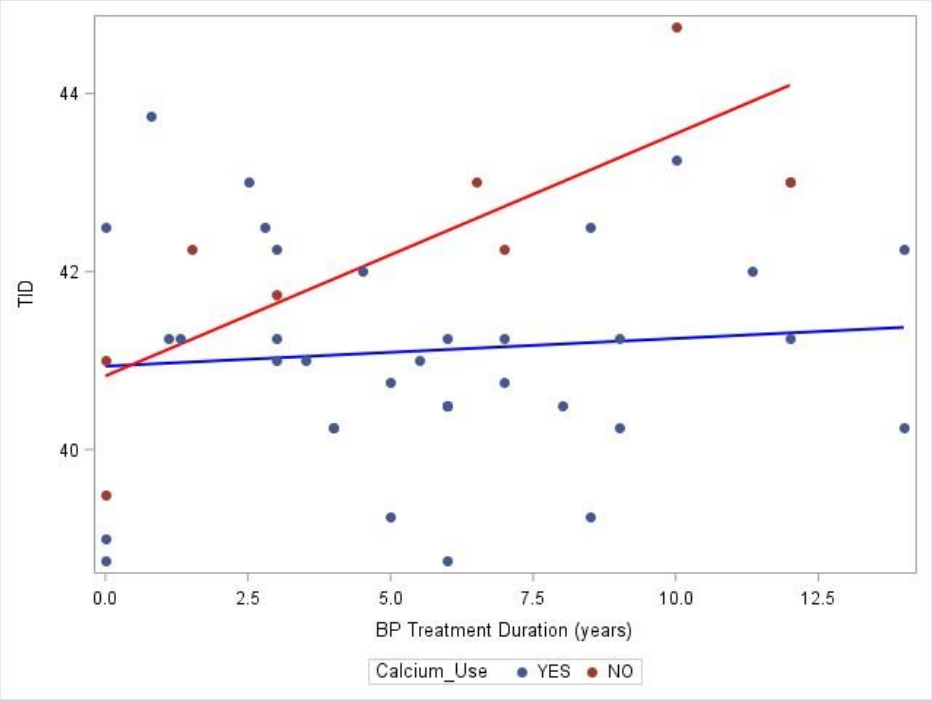

Figure 3.13 TID vs Treatment Duration Considering Calcium Usage

3.4 Discussion

RPI parameters can be sorted into to two categories based upon how the parameter is calculated. All RPI parameters are calculated by measuring either test probe displacement (indentation depth parameters) or the relationship between force and test probe displacement (loading/unloading slope parameters). Both of these categories include RPI parameters which were shown by the results of the present study to be significantly correlated with bisphosphonate treatment duration. Because these parameters and have also been related to established material properties, the results of the present study provide evidence that the material properties of trabecular bone are related to bisphosphonate treatment duration. The three indentation depth parameters correlated positively with bisphosphonate treatment length while the three loading/unloading slope parameters negatively correlated with bisphosphonate treatment length. An RPI parameter's significance with bisphosphonate treatment length was found to be generally affected by which indentation cycle(s) were used in the calculation of the RPI parameter.

3.4.1 Indentation Depth with Increasing Treatment Duration

The indentation distance between the first indentation cycle and last indentation cycle increased with increasing bisphosphonate treatment duration. A similar trend was seen in outputs of ED and TID. ED is a function of TID and the force applied over time. The force produced by the indentation probe is consistent for each indentation, therefore ED is directly related to TID due to ED's calculation method. This explains similar ED and TID p-values (p=0.049 and 0.049 respectively) and multiple regression coefficients seen in .

Table 3.1.

First cycle indentation depth was the only indentation depth parameter that was unrelated to bisphosphonate treatment duration. The particular locations at which an indent was placed may contain varying amounts of physical imperfections such as microcracks or surface imperfections. The 1st cycle indentation depth deforms the most bone volume. The calculations for ED and TID take the 1st cycle indentation depth measurement into account. Physical material imperfections may have contributed to the higher data variability seen in ED (p=0.049) and TID (p=0.049) compared to another indentation depth parameter that doesn't take 1st cycle indentation depth into account (p=0.01 for IDI). Three of the four RPI indentation parameters (TID, ID1st, IDI, and ED) each calculated using indentation depth, showed significant positive relationships with bisphosphonate treatment duration. These parameters reflect changes in the material properties of bone associated with varying bisphosphonate treatment duration.

3.4.2 Indentation Depth and Material Properties

IDI has been shown in other studies to be inversely proportional to yield stress, strength, and toughness as measured by traditional destructive mechanical tests [37] [30] [35] [36] [33]. Güerri-Fernández et al. found significantly higher TID and IDI in fractured, long-term bisphosphonate treated patients compared to osteoporotic control patients [30] (Figure 3.14 A and B).

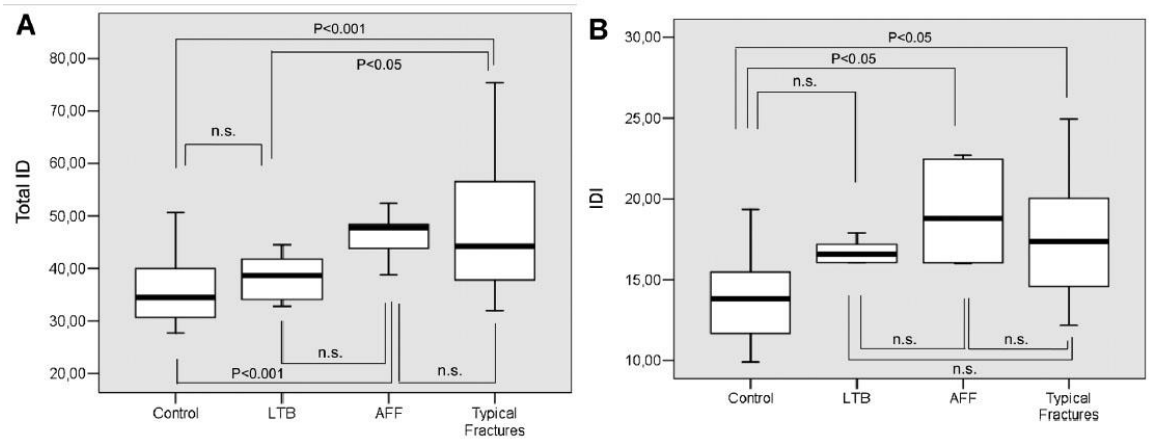

Figure 3.14 A & B Results of Güerri-Fernández et al. [30]

Aref et al. studied beagles treated with bisphosphonates for 6 months and found a decrease in IDI and ED when indenting beagle ribs compared ribs taken from untreated beagles [34]. Discrepancy between the presently observed increases in IDI and ED with increasing bisphosphonate treatment duration in human bone and the decreased IDI and ED observed in beagles following 6 months of bisphosphonate treatment may be due to the single brief treatment duration of the beagle study compared to the lengthy (0.3 to 14 years) treatment durations used in the present study.

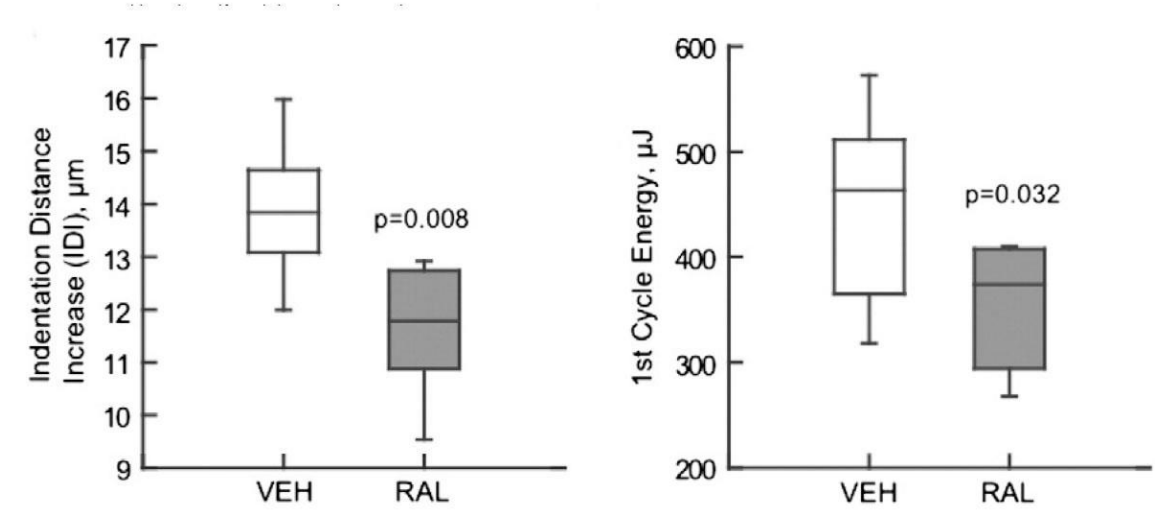

Figure 3.15 Comparing control (VEH) and BP treated (RAL) beagle by Aref et al. [34]

Nogués et al. used a similar RPI device which outputs a different parameter than the RPI device in the present study [42]. Nevertheless, Nogués et al. found a significant decrease in the bone material strength index, the single output parameter of their RPI device, in 40 long-term treated patients treated with bisphosphonates for 4-14 years [42]. Gallant et al. found that healthy beagles treated with bisphosphonates for three years showed a significant increase in cortical rib IDI compared to untreated control beagles (Figure 3.16) [35]. Gallant et al. also was able to correlate their IDI results to bone toughness as measured by three-point bending testing of excised beagle ribs [35].

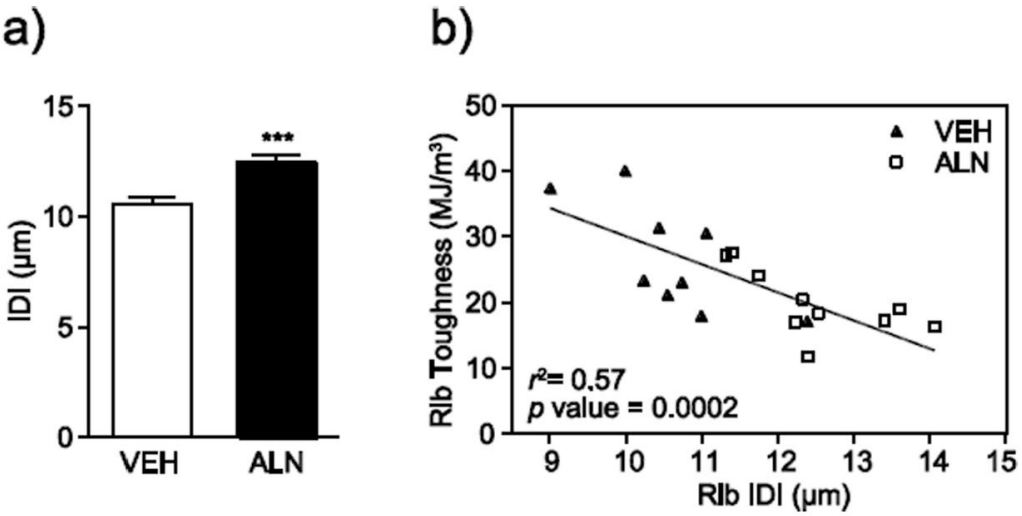

Figure 3.16 Results of Gallant et al. [35]

3.4.3 Loading/Unloading Slope with Increasing Treatment Duration

The present study showed that RPI parameters involving loading and unloading portions of the force-depth indentation cycle were related to bisphosphonate treatment duration. Multiple regression models relating AvgUS, US1st, and AvgLS to treatment duration, following the inclusion of age and calcium supplementation as covariates, all showed negative slopes in the expressions relating the dependent variable (RPI parameters) to the independent variable (treatment duration). Unloading slope, not loading slope, is traditionally used in other indentation methods to calculate elastic modulus of a material [22] [23]. Like the RPI indentation depth measurements, the loading/unloading slope output parameters of the RPI device are indications of well-established material properties.

3.4.4 Loading/Unloading Slope and Material properties

Gallant et al. found significantly lower values of US1st in diabetic rat femurs and vertebrae compared to a nondiabetic control group [35]. US1st has been associated with material properties derived from rat vertebral axial compression testing such as toughness and modulus [35].

3.4.5 Correlated RPI Parameters and Trabecular Bone Mechanical Properties

Studies comparing RPI parameters to traditional mechanical properties the idea that increases in IDI, TID, and ED and decreases in AvgUS, US1st, and AvgLS indicate a decrease in a material's yield stress, strength, and toughness. The presently observed increases in IDI, TID, and ED with increasing BP treatment duration indicate a decline in the material properties of trabecular bone with increasing bisphosphonate treatment duration. If loading and unloading slope RPI parameters (AvgUS, US1st, and AvgLS) are in fact indicators of modulus and toughness, as found by Gallant et al., then the present study's results show a decline in trabecular bone modulus and toughness with increasing bisphosphonate treatment.

3.5 Uncorrelated RPI Parameters

Three parameters (CID, CID1st, and ID1st) were uncorrelated with bisphosphonate treatment duration. Two of these parameters, CID and CID1st, are creep-related and measure changes in probe displacement during constant load application. This lack of significance may be a result of the selected device loading frequency of 2 Hertz and bone sample preparation. Dehydrated bone is known to have decreased viscoelastic properties, increased material modulus, and increased microhardness as measured by nanoindentation [43]. Creep related RPI measurements are less sensitive in dry bone and thus less able to detect changes associated with bisphosphonate duration. The length of time in which a constant force is applied before the device takes a creep-related RPI measurement is short. Specifically, the present study used an indentation frequency of 2 Hz resulting in a constant force being applied to the sample for 0.167 seconds for each indentation cycle as shown in Figure 3.17. Other nanoindentation studies using dehydrated cortical bone apply constant load loading for 30 to 60 seconds to measure material creep properties accurately [50] [44] [45]. Relatively short loading

durations from the RPI device, and the use of dehydrated bone samples, decreased the magnitude of RPI creep parameters to the extent that RPI creep parameter magnitudes were comparable in size to the measurement uncertainty of the RPI device. This similarity reduced the likelihood of detecting a significant correlation.

The remaining RPI parameter, 1st cycle indentation depth (ID1st), was unrelated to BP treatment duration even when considering patient age and calcium supplementation as covariates (p=0.088). The ID1st parameter is directly affected by physical imperfections in the volume of bone it deforms. The initial indentation produces the largest plastic deformation of all cycles (Figure 3.18 and Figure 3.19). Therefore first cycle indentation depth is the RPI parameter most likely to be affected by material variances within a volume. Even though many of these imperfections are on the level of nanometers, altering TID a single micron is a 2.2-3.8% measurement variation. For comparison, a study by Granke, et al. found the variation for TID on a homogeneous, calibrated surface to be 0.8% [36].

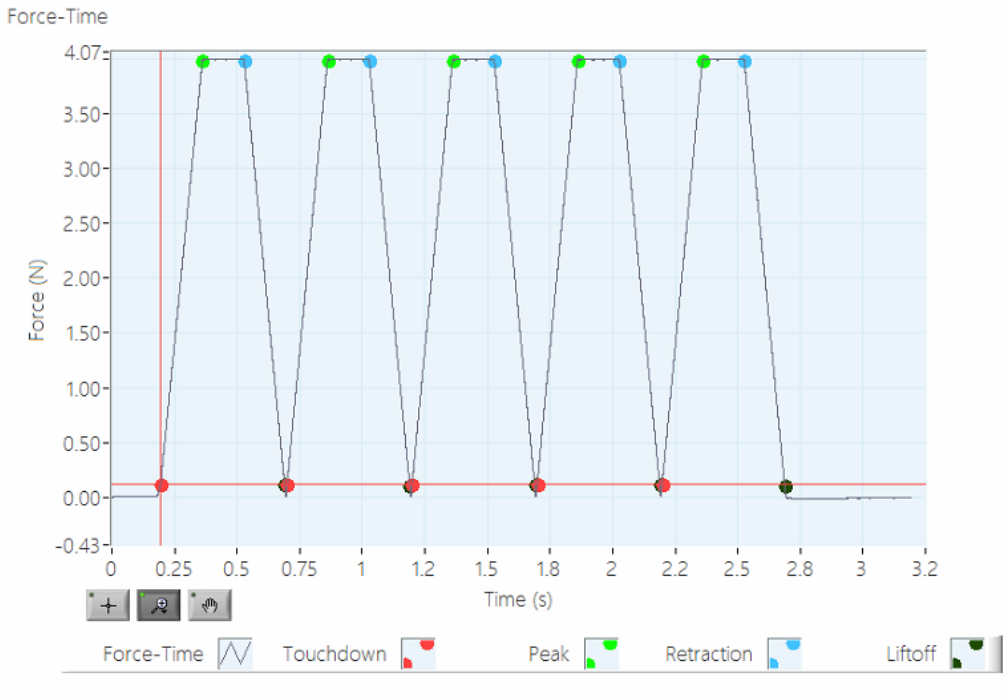

Figure 3.17 Force-Time Graph of a 4 N 5 Cycle Indent at 2 Hz

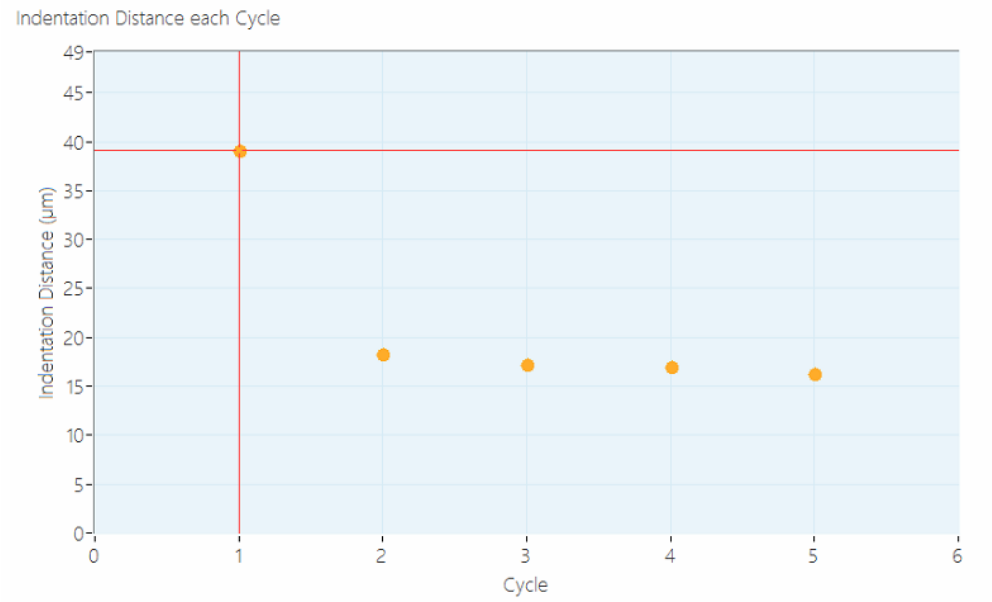

Figure 3.18 Indentation Distance per Cycle

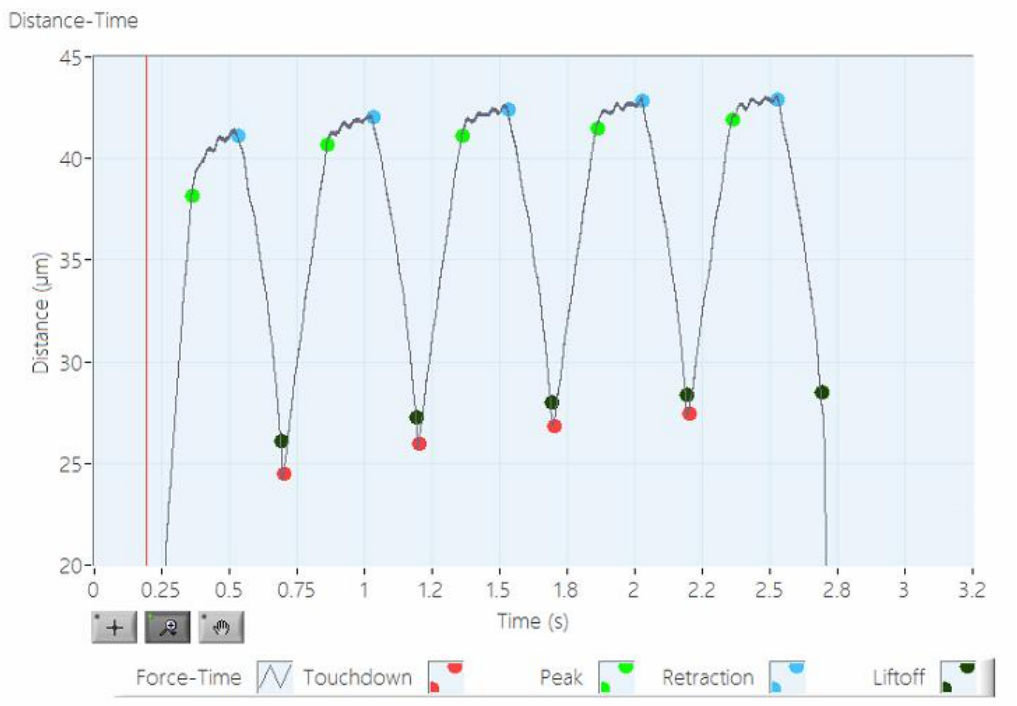

Figure 3.19 Distance-Time Graph of a 4 N, 5 Cycle, and 2 Hz RPI

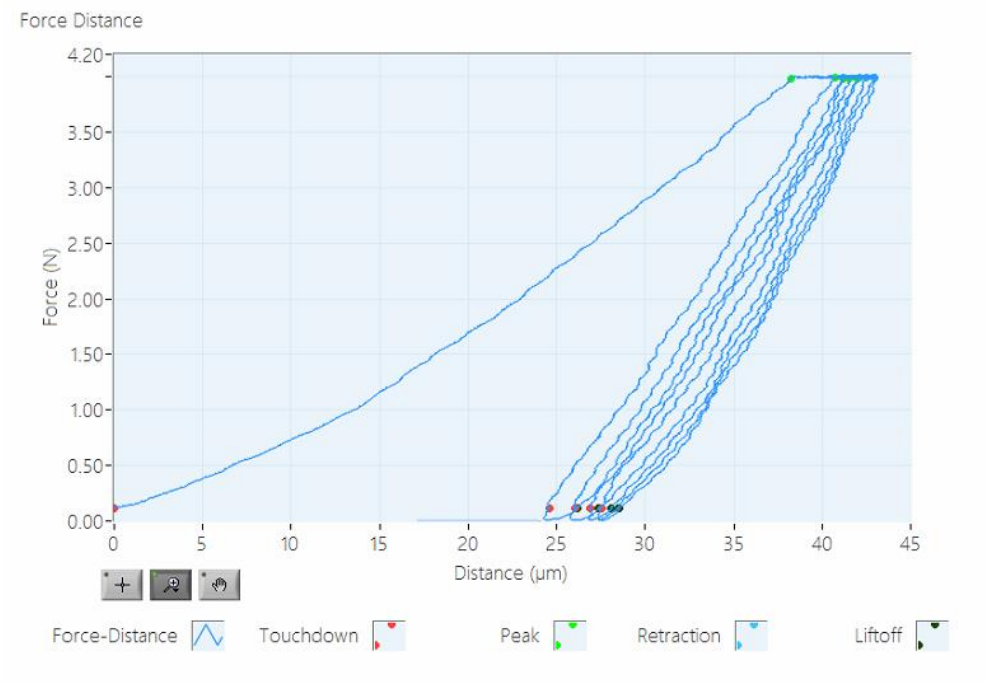

Figure 3.20 Force-Distance Graph of a 4 N, 5 Cycle, and 2 Hz RPI

3.5.1 Calcium Supplement Usage

Subjects who did not report use of calcium supplements showed greater rates of change in IDI and TID with bisphosphonate treatment duration compared to subjects who reported use of calcium supplements. A rigorous comparison cannot be made between these two populations because the number of patients in the present study not taking a calcium supplement (7 patients) is substantially less than patients who did (35 patients). The increased TID and IDI slopes of bisphosphonate treated individuals not taking a calcium supplement indicates an accelerated decrease in trabecular bone yield stress, strength, and toughness versus bisphosphonate treated patients taking a calcium supplement [13]. Alternatively, decreased TID and IDI slopes of bisphosphonate treated individuals taking a calcium supplement may indicate that calcium supplementation decreases the rate at which trabecular bone yield stress, strength, and toughness deteriorates versus bisphosphonate treated patients not taking a calcium supplement [13]. It is also possible that patients not taking a calcium supplement have a higher likelihood of noncompliant bisphosphonate usage which would result in an accelerated decrease in trabecular bone property compared to compliant patients [13].

3.5.2 Limitations

The linear regression of all BioDent parameters with treatment duration showed a low R-Square value despite significant p values. There is an inherently high variability between samples based upon unknown contributing factors inherent to cross sectional studies.

Bone biopsies selected for this test were all supplied by the University of Kentucky Division of Nephrology bone library. The inclusion and exclusion criteria used to select samples were based on available patient information. Patient information was not comprehensive and some data remain unknown. For example, a patient may have claimed to have exercised regularly but the degree and type of exercise was not noted. Accuracy of patient reported information is not assured and no guarantees exist that patients were completely compliant with their BP treatment.

The shape and size of the substrate beneath the exposed surface of the biopsy was unknown for each indent. Indentations with visual abnormalities or measurements resembling PMMA were discarded as discussed in section 3.2.4. It is possible that indents partially interacting with PMMA because of insufficient substrate volume were analyzed in the results.

4 Conclusions

4.1 Reference Point Indentation of Trabecular Bone

Reference point indentation can be successfully used to quantify relevant material parameters of trabecular human bone. The protocol developed for RPI study of such bone, i.e., indents of 4 N and 5 cycles applied to two indentation sites in each of two randomly chosen trabeculae per each bone sample, was proven feasible and minimizes data variability when applied to large numbers of bone samples obtained from a diverse patient population.

4.2 Relevance of Material Property Changes in Trabecular Bone

Increasing bisphosphonate treatment duration is associated with reductions in trabecular bone modulus, yield stress, strength, and toughness as reflected by RPI related

parameters. The relevance of these RPI parameters to well established material parameters of modulus, yield stress, strength, and toughness are supported by previously published studies. RPI's ability to indicate material parameters changes may offer new opportunities for treatment monitoring. These opportunities may lead to new guidelines for bisphosphonate treatment discontinuance or to assess the effectiveness of other treatment options to change bone material properties and subsequently the mechanical load bearing competence of bone.

4.3 Future Directions

4.3.1 Calcium Supplementation

Comparatively higher rates of increase in IDI and TID in patients not reportedly taking calcium supplements during bisphosphonate treatment indicates that this treatment group experienced a higher rate of material property deterioration compared to those taking a calcium supplement as discussed in section 3.5.1. Patients in this study who reported taking calcium supplements were observed to have comparatively lower rates of trabecular bone material property deterioration with increasing bisphosphonate treatment duration as indicated by TID and IDI. Alternatively, it could be inferred that patients who use a calcium supplement take greater personal responsibility for their bone health and are more compliant with their bisphosphonate treatment and thus have more favorable trabecular bone material properties, as indicated by RPI parameters, because bisphosphonates are efficacious when taken as prescribed. Evaluation of this hypothesis awaits further study. A larger cross sectional study may provide some clarifying information that helps reduce data variations due to possible patient noncompliance.

4.3.2 Nanoindentation Comparison

Reference point indentation parameters are relatively unproven in comparison to established material parameters such as Young's modulus, yield point, strength, etc. that are obtained from conventional destructive material testing. All bone samples indented with the RPI device in the present study have also been indented using a Nanoindenter XP (MTS Nano Instruments, Oak Ridge, TN) to measure Young's modulus and microhardness. The usefulness of one or more of the nine studied RPI parameters will be

strengthened if correlations are observed between one or more of these parameters and Young's modulus or hardness as measured by nanoindentation.

4.3.3 Cortical Bone RPI

The first objective of this study was to pioneer the use of RPI within trabecular bone. Some trabecular bone biopsies indented in the present study also contain cortical bone suitable for reference point indentation. Taking RPI measurements of this cortical bone despite its small sample size is merited given the successful technique development and significant correlations between 6 of 9 RPI parameters and varying bisphosphonate treatment. Comparisons between the RPI parameters of different mineralized tissue types (cortical and trabecular) within the same sample could be investigated.

Appendices

Appendix A: SAS Output

The SAS System

The GLM Procedure

Dependent Variable: m_IDI IDI

Source	DF	Sum of Squares	Mean Square	F Value	Pr > F
Model	3	2.41449600	0.80483200	6.97	0.0007
Error	40	4.62202389	0.11555060		
Corrected Total	43	7.03651989			

R-Square	Coeff Var	Root MSE	m_IDI Mean
0.343138	8.098986	0.339927	4.197159

Source	DF	Type I SS	Mean Square	F Value	Pr > F
age	1	0.00425422	0.00425422	0.04	0.8488
calcium	1	1.03566425	1.03566425	8.96	0.0047
dur	1	1.37457753	1.37457753	11.90	0.0013

Source	DF	Type III SS	Mean Square	F Value	Pr > F
age	1	0.22529821	0.22529821	1.95	0.1703
calcium	1	1.30151527	1.30151527	11.26	0.0017
dur	1	1.37457753	1.37457753	11.90	0.0013

Parameter	Estimate	Standard Error	t Value	Pr > |t|
Intercept	4.906973072	0.44891197	10.93	<.0001
age	-0.009797848	0.00701678	-1.40	0.1703
calcium	-0.451042684	0.13439376	-3.36	0.0017
dur	0.046788057	0.01356552	3.45	0.0013

The GLM Procedure

Dependent Variable: m_AvgLS AvgLS

Source	DF	Sum of Squares	Mean Square	F Value	Pr > F
Model	3	0.00056166	0.00018722	1.90	0.1456
Error	40	0.00394800	0.00009870		
Corrected Total	43	0.00450966			

R-Square	Coeff Var	Root MSE	m_AvgLS Mean
0.124545	4.499545	0.009935	0.220795

Source	DF	Type I SS	Mean Square	F Value	Pr > F
age	1	0.00001499	0.00001499	0.15	0.6988
calcium	1	0.00013786	0.00013786	1.40	0.2442
dur	1	0.00040880	0.00040880	4.14	0.0485

Source	DF	Type III SS	Mean Square	F Value	Pr > F
age	1	0.00010495	0.00010495	1.06	0.3087
calcium	1	0.00019324	0.00019324	1.96	0.1695
dur	1	0.00040880	0.00040880	4.14	0.0485

Parameter	Estimate	Standard Error	t Value	Pr > |t|
Intercept	0.2077937786	0.01312000	15.84	<.0001
age	0.0002114664	0.00020507	1.03	0.3087
calcium	0.0054959110	0.00392782	1.40	0.1695
dur	-.0008068786	0.00039647	-2.04	0.0485

The GLM Procedure

Dependent Variable: m_TID TID

Source	DF	Sum of Squares	Mean Square	F Value	Pr > F
Model	3	15.59834135	5.19944712	3.22	0.0328
Error	40	64.66728365	1.61668209		
Corrected Total	43	80.26562500			

R-Square	Coeff Var	Root MSE	m_TID Mean
0.194334	3.077732	1.271488	41.31250

Source	DF	Type I SS	Mean Square	F Value	Pr > F
age	1	0.84049497	0.84049497	0.52	0.4751
calcium	1	8.09556885	8.09556885	5.01	0.0309
dur	1	6.66227752	6.66227752	4.12	0.0490

Source	DF	Type III SS	Mean Square	F Value	Pr > F
age	1	3.40899190	3.40899190	2.11	0.1543
calcium	1	9.68907319	9.68907319	5.99	0.0188
dur	1	6.66227752	6.66227752	4.12	0.0490

Parameter	Estimate	Standard Error	t Value	Pr > |t|
Intercept	44.09260007	1.67914191	26.26	<.0001
age	-0.03811227	0.02624606	-1.45	0.1543
calcium	-1.23064879	0.50269588	-2.45	0.0188
dur	0.10300582	0.05074143	2.03	0.0490

The GLM Procedure

Dependent Variable: m_ED ED

Source	DF	Sum of Squares	Mean Square	F Value	Pr > F
Model	3	9.77007515	3.25669172	2.19	0.1041
Error	40	59.45110383	1.48627760		
Corrected Total	43	69.22117898			

R-Square	Coeff Var	Root MSE	m_ED Mean
0.141143	11.97694	1.219130	10.17898

Source	DF	Type I SS	Mean Square	F Value	Pr > F
age	1	0.00040943	0.00040943	0.00	0.9868
calcium	1	3.22969821	3.22969821	2.17	0.1483
dur	1	6.53996751	6.53996751	4.40	0.0423

Source	DF	Type III SS	Mean Square	F Value	Pr > F
age	1	0.76817953	0.76817953	0.52	0.4764
calcium	1	4.27814259	4.27814259	2.88	0.0975
dur	1	6.53996751	6.53996751	4.40	0.0423

Parameter	Estimate	Standard Error	t Value	Pr > |t|
Intercept	11.38855347	1.60999695	7.07	<.0001
age	-0.01809186	0.02516528	-0.72	0.4764
calcium	-0.81775016	0.48199549	-1.70	0.0975
dur	0.10205592	0.04865196	2.10	0.0423

The GLM Procedure

Dependent Variable: m_AvgUS AvgUS

Source	DF	Sum of Squares	Mean Square	F Value	Pr > F
Model	3	0.00203197	0.00067732	3.01	0.0412
Error	40	0.00899303	0.00022483		
Corrected Total	43	0.01102500			

R-Square	Coeff Var	Root MSE	m_AvgUS Mean
0.184305	4.798141	0.014994	0.312500

Source	DF	Type I SS	Mean Square	F Value	Pr > F
age	1	0.00001984	0.00001984	0.09	0.7680
calcium	1	0.00044477	0.00044477	1.98	0.1673
dur	1	0.00156736	0.00156736	6.97	0.0118

Source	DF	Type III SS	Mean Square	F Value	Pr > F
age	1	0.00028469	0.00028469	1.27	0.2672
calcium	1	0.00064158	0.00064158	2.85	0.0989
dur	1	0.00156736	0.00156736	6.97	0.0118

Parameter	Estimate	Standard Error	t Value	Pr > |t|
Intercept	0.2917207094	0.01980150	14.73	<.0001
age	0.0003482896	0.00030951	1.13	0.2672
calcium	0.0100142836	0.00592811	1.69	0.0989
dur	-.0015799204	0.00059838	-2.64	0.0118

The GLM Procedure

Dependent Variable: m_US1st US1st

Source	DF	Sum of Squares	Mean Square	F Value	Pr > F
Model	3	0.00141269	0.00047090	2.09	0.1161
Error	40	0.00899129	0.00022478		
Corrected Total	43	0.01040398			

R-Square	Coeff Var	Root MSE	m_US1st Mean
0.135784	4.852376	0.014993	0.308977

Source	DF	Type I SS	Mean Square	F Value	Pr > F
age	1	0.00000435	0.00000435	0.02	0.8901
calcium	1	0.00024540	0.00024540	1.09	0.3024
dur	1	0.00116294	0.00116294	5.17	0.0284

Source	DF	Type III SS	Mean Square	F Value	Pr > F
age	1	0.00015893	0.00015893	0.71	0.4054
calcium	1	0.00037375	0.00037375	1.66	0.2046
dur	1	0.00116294	0.00116294	5.17	0.0284

Parameter	Estimate	Standard Error	t Value	Pr > |t|
Intercept	0.2943424440	0.01979958	14.87	<.0001
age	0.0002602301	0.00030948	0.84	0.4054
calcium	0.0076433972	0.00592753	1.29	0.2046
dur	-.0013609105	0.00059832	-2.27	0.0284

REFERENCES

[1] R. Baron, "Anatomy and Ultrastructure of Bone," in *Primer on the Metabolic Bone Diseases and Disorders of Mineral Metabolism*, Philadelphia, Lippincott Williams & Wilkins, 1999, pp. 3-10.

[2] J. Currey, "Effects of Differences in Mineralization on the Mechanical Properties of Bone," *Philosophical Transactions of the Royal Society*, vol. 304, no. 1121, pp. 509-518, 1984.

[3] S. A. Krum and M. Brown, "Unraveling estrogen action in osteoporosis," *Cell Cycle*, vol. 7, no. 10, pp. 1348-1352, 2008.

[4] Y. Bala, D. Farlay, R. Chapurlat and G. Boivin, "Modifications of bone material properties in postmenopausal osteoporotic women long-term treated with alendronate," *Eur J Endocrinol*, vol. 165, no. 4, pp. 647-55, 2011.

[5] O. Johnell, D. Marchall and H. Wedel, "Meta-analysis ofhow well measures of bone mineral density predict occurrence of osteoporotic fractures," *BMJ*, no. 1254, p. 312, 1996.

[6] T. Topolinsk, A. Mazurkiewicz, S. Jung, A. Cichanski and K. Nowicki, "Microarchitecture Parameters Describe Bone Structure and Its Strength Better Than BMD," *The Scientific World Journal*, vol. 2012, no. 502781, pp. 1-7, 2012.

[7] P. Delmas and E. Seeman, "Changes in bone mineral density explain little of the reduction in vertebral or nonvertebral fracture risk with anti-resorptive therapy," *Bone*, vol. 34, no. 4, pp. 599-604, 2004.

[8] M. R. Allen, K. Iwata, M. Sato and B. D, "Raloxifene enhances vertebral mechanical properties independent of bone density," *Bone*, vol. 39, no. 5, pp. 1130-1135, 2006.

[9] J. Compston, "Bone quality: what is it and how is it measured?," *Arquivos Brasileiros de Endocrinologia e Metabologia*, vol. 50, no. 4, pp. 579-585, 2006.

[10] K. Faulkner, "Bone matters: are density increases necessary to reduce fracture risk?," *J Bone Miner Res.*, vol. 15, pp. 183-187, 2000.

[11] R. Burge, B. Dawson-Hughes, D. H. Solomon, J. B. Wong and A. King, "Incidence and Economic Burden of Osteoporosis-Related Fractures in the United States, 2005–2025," *Journal of Bone and Mineral Research*, pp. 22:465-475, 2007.

[12] S. W. Blume and J. R. Curtis, "Medical costs of osteoporosis in the elderly Medicare population," *Osteoporosis International*, vol. 22, no. 6, pp. 1835-1844, 2011.

[13] M. J. Benton and A. White, "Osteoporosis: Recommendations for Resistance Exercise and Supplementation With Calcium and Vitamin D to Promote Bone Health," *Journal of Community Health Nursing*, vol. 4, no. 23, pp. 201-211, 2006.

[14] P. Salari Sharif, A. M. and B. Larijani, "Current, new and future treatments of osteoporosis," *Rheumatology International,* vol. 31, no. 3, pp. 289-300, 2011.

[15] A. D. A. C. o. S. Affairs, "Dental Management of Patients Receiving Oral Bisphosphonate Therapy," *Journal of the American Dental Assocation,* vol. 137, no. 8, pp. 1144-50, 2006.

[16] L. Plotkin, R. Weinstein, A. Parfitt, P. Roberson, S. Manolagas and T. Bellido, "Prevention of osteocyte and osteoblast apoptosis by bisphosphonates and calcitonin," *J Clin Invest,* vol. 104, no. 10, pp. 1363-74, 1999.

[17] D. MT, C. BL and K. S., "Bisphosphonates: mechanism of action and role in Clinical Practice," *Mayo Clin Proc,* vol. 83, no. 9, pp. 1032-45, 2008.

[18] D. B. Burr, M. R. Forwood, D. P. Fyhrie, B. R. Martin, M. B. Schaffler and C. H. Turner, " Bone Microdamage and Skeletal Fragility in Osteoporotic and Stress Fractures," *JOURNAL OF BONE AND MINERAL RESEARCH,* vol. 12, no. 1, pp. 6-15, 1997.

[19] M. Swiontkowski and L. Resnick, "Treating Atypical Femoral Fractures Related to Bisphosphonates," *JBJS Case Connect,* vol. 5, no. 1, p. e5, 2015.

[20] M. Swiontkowski and L. Resnick, "Atypical Femoral Fractures," *JBJS Case Connect,* vol. 6, no. 1, p. e4, 2016.

[21] O. Jiroušek, "Nanoindentation of Human Trabecular Bone – Tissue Mechanical Properties Compared to Standard Engineering Test Methods," in *Nanoindentation in Materials Science,* InTech, 2012, pp. 259-284.

[22] W. Oliver and G. Pharr, "An improved technique for determining hardness and elastic modulus using load and displacement sensing indentation experiments," *Journal of Materials Research,* vol. 7, no. 6, pp. 1564-1583, 1992.

[23] G. Pharr, "Measurement of mechanical properties by ultra-low load indentation," *Measurement of mechanical properties by ultra-low load indentation,* vol. 253, no. 1-2, pp. 151-159, 1998.

[24] G. Pharr, W. Oliver and F. Brotzen, "On the generality of the relationship among contact stiffness, contact area, and the elastic modulus during indentation," *Journal of Materials Research,* vol. 7, no. 3, pp. 613-617, 1992.

[25] J. Rho, T. Tsui and G. Pharr, "Elastic properties of human cortical and trabecular lamellar bone measured by nanoindentation," *Biomaterials,* vol. 28, no. 20, pp. 1325-1330, 1997.

[26] P. Zysset, X. Guo, C. Hoffler, K. Moore and S. Goldstein, "Elastic modulus and hardness of cortical and trabecular bone lamellae measured by nanoindentation in the human femur," *Journal of Biomechanics,* vol. 32, no. 10, pp. 1005-1012, 1999.

[27] J. Rho, M. 2. Roym, T. Tsui and P. GM, "Elastic properties of microstructural components of human bone tissue as measured by nanoindentation," *Journal of Biomedical Materials Research,* vol. 45, no. 1, pp. 48-54, 1999.

[28] C. Hoffler, K. Moore, K. Kozloff, P. Zysset, M. Brown and S. Goldstein, " Heterogeneity of bone lamellar-level elastic moduli," *Bone,* vol. 26, no. 6, pp. 603-609, 2000.

[29] S. Hengsberger, A. Kulik and P. Zysset, "Nanoindentation discriminates the elastic properties of individual human bone lamellae under dry and physiological conditions," *Bone,* vol. 30, no. 1, pp. 178-184, 2002.

[30] R. Güerri-Fernández, X. Nogués, J. M. Quesada Gómez, E. Torres del Pliego, L. Puig, N. García-Giralt, G. Yoskovitz, L. Mellibovsky, P. K. Hansma and A. Díez-Pérez, "Microindentation for in vivo measurement of bone tissue material properties in atypical femoral fracture patients and controls," *JBMR,* vol. 28, no. 1, pp. 162-168, 2012.

[31] ActiveLife Scientific, "Reference Point Indentation: Research Guide," Santa Barbara, 2015.

[32] A. Carriero, J. Bruse, K. Oldknow, J. L. Millán, C. Farquharson and S. J. Shefelbinea, "Reference point indentation is not indicative of whole mouse bone measures of stress intensity fracture toughness," *Bone,* vol. 69, pp. 174-179, 2014.

[33] O. Katsamenis, T. Jenkins and P. Thurner, "Toughness and damage susceptibility in human cortical bone is proportional to mechanical inhomogeneity at the osteonal-level.," *Bone,* vol. 76, pp. 158-168, 2015.

[34] M. Aref, M. A. Gallanta, J. M. Organa, J. M. Wallaceb, C. L. Newmana, D. Burr, B. D. M. and M. R. Allena, "In vivo reference point indentation reveals positive effects of raloxifene on mechanical properties following 6 months of treatment in skeletally mature beagle dogs," *Bone,* vol. 56, no. 2, 2013.

[35] M. A. Gallant, D. M. Brown, J. M. Organ, M. R. Allen and D. B. Burr, "Reference-Point Indentation Correlates with Bone Toughness Assessed Using Whole-Bone Traditional Mechanical Testing," *Bone,* vol. 53, no. 1, pp. 301-305, 2013.

[36] M. Granke, A. Coulmier, S. Uppuganti, J. Gaddy, M. Does and J. Nyman, "Insights into Reference Point Indentation Involving Human Cortical Bone: Sensitivity to Tissue Anisotropy and Mechanical Behavior," *Journal of the Mechanical Behavior of Biomedical Materials,* vol. 37, pp. 174-185, 2014.

[37] A. Diez-Perez, R. Güerri, X. Nogues, E. Cáceres, M. J. Peña, L. Mellibovsky, C. Randall, D. Bridges, J. C. Weaver and A. Proctor, "Microindentation for in vivo measurement of bone tissue mechanical properties in humans," *Journal of Bone and Mineral Research,* vol. 25, no. 8, pp. 1877-1885, 2010.

[38] O. Katsamenis, T. Jenkins and P. Thurner, "Toughness and damage susceptibility in human cortical bone is proportional to mechanical inhomogeneity at the osteonal-level," *Bone,* vol. 76, pp. 158-168, 2015.

[39] A. B. H. O. T. B. O. T. F. E. METHOD, "Gupta, K. K.; Meed, J. L.," *International Journal for Numberical Methods in Engineering,* vol. 39, pp. 3761-3774, 1996.

[40] P. K. Zysset, E. Guo, E. Hoffler, K. E. Moore and S. Goldstein, "Elastic Modulus and Hardness of Cortical and Trabecular Bone Lamellae Measured by Nanoindentation in the Human Femur," *Journal of Biomechanics,* vol. 32, no. 10, pp. 1005-1012, 1999.

[41] C. Tjhiaa, C. V. Odvinac, D. S. Raod, S. M. Stovere, X. Wanga and D. Fyhriea, "Mechanical property and tissue mineral density differences among severely suppressed bone turnover (SSBT) patients, osteoporotic patients, and normal subjects," *Bone,* vol. 49, no. 6, pp. 1279-1289, 2011.

[42] X. Nogués, D. Prieto-Alhambra, R. Güerri-Fernández, L. Mellibovsky and A. Diez-Perez, "Restoring bone tissue quality: a treatment target in long-term bisphosphonate therapy?," *ECTS-IBMS Abstracts* , p. P26, 2015.

[43] S. Ferreri, B. Hu and Y. Qin, "The effects of dehydration on elastic and viscoelastic material properties obtained using nanoindentation," *Transactions of the 56th annual meeting of the ORS,* p. 628, 2010.

[44] W. Ziheng, B. Tyler A., O. Timothy C. and N. Glen L., "The Effect of Holding Time on Nanoindentation Measurements of Creep in Bone," *J Biomech,* vol. 44, no. 6, pp. 1066-1072, 2011.

[45] H. Isaksson, M. Malkiewicz, R. Nowak, H. J. Helminen and J. S. Jurvelin, "Rabbit cortical bone tissue increases its elastic stiffness but becomes less viscoelastic with age," *Bone,* vol. 47, no. 6, pp. 1030-1038, 2010.

[46] A. o. A. (AoA), "Profile of Older Americans:2014 Profile," 2014. [Online]. Available: http://www.aoa.acl.gov/Aging_Statistics/Profile/2014/4.aspx. [Accessed 1 January 2016].

[47] D. Sellmeyer, "Atypical fractures as a potential complication of long-term bisphosphonate therapy.," *JAMA,* vol. 304, no. 13, pp. 1480-4, 2010.

[48] J. Schilcher, K. Muchaelsson and P. Aspenberg, "Bisphosphonate Use and Atypical Fractures of the Femoral Shaft," *The New England Journal of Medicine,* vol. 362, no. 18, pp. 1728-37, 2011.

[49] T. Yli-Kyyny, I. Tamminen and H. A. Kroger, "Atraumatic bilateral femur fracture in long-term bisphosphonate use," *Orthopedics,* vol. 33, no. 12, p. 867, 2010.

[50] D. Bauer, "Bisphosphonate Use and Atypical Femoral Fractures: Getting Down to

Brass Tacks," *J Clin Endocrinol Metab,* vol. 95, no. 12, pp. 5207-529, 2010.

[51] D. Porter, "The Effect of Various Pathologies on Bone Quality," .*Theses and Dissertations--Biomedical Engineering,* p. Paper 15, 2014.

[52] J. Zhang, G. L. Niebur and T. C. Ovaert, "Mechanical property determination of bone through nano- and micro-indentation testing and finite element simulation," *Journal of Biomechanics,* vol. 41, no. 2, pp. 267-275, 2007.

[53] P. Roschger, E. Paschalis, P. Fratzl and K. Klaushofer, "Bone mineralization density distribution in health and disease," *Bone,* vol. 42, no. 3, pp. 456-466, 2008.

[54] G. Dumas and C. Baronet, "Elastoplastic indentation of a half-space by an infinitely long rigid circular cylinder," *International Journal of Mechanical Sciences,* vol. 13, no. 6, pp. 519-530, 1971.

[55] C. Hardy, C. Baronet and G. Tordion, " Indentation of an elastic-perfectly-plastic half-space by a hard sphere," *Journal of Basic Engineeing,* vol. 94, no. 1, pp. 251-253, 1972.

[56] Y. Cheng and C. Cheng, " Scaling Relationships in Conical Indentation of Elastic Perfectly Plastic Solids," *Journal of Solid Structures,* vol. 36, pp. 1231-1243, 1999.

[57] O. Brennan, O. Kennedy, T. Lee, S. Rackard and F. O'Brien, "Biomechanical properties across trabeculae from the proximal femur of normal and ovariectomised sheep," *Journal of Biomechanics,* vol. 42, no. 4, pp. 498-503, 2009.

[58] W. Leslie, S. Majumdar, S. Morin and L. Lix, "Why does rate of bone density loss not predict fracture risk?," *J Clin Endocrinol Metab.,* vol. 100, no. 2, pp. 679-683, 2015.

[59] D. Marshall, O. Johnell and H. Wedel, "Meta-analysis of how well measures of bone mineral density predict occurrence of osteoporotic fractures," *BMJ,* vol. 213, no. 7041, pp. 1254-9, 1996.

[60] T. Lee, S. Mohsin, D. Taylor, R. Parkesh, T. Gunnlaugsson, F. O'Brien and e. al., "Detecting microdamage in bone," *J Anat,* vol. 203, pp. 161-172, 2003.

[61] M. E. Launey, M. J. Buehler and R. O. Ritchie, "On the mechanistic origins of toughness in bone," *Ann. Rev. Mater. Res.,* vol. 40, pp. 25-53, 2010.

[62] D. Burr, "Why bones bend but don't break," *J Musculosckelet Neuronal Interact.,* vol. 11, no. 4, pp. 270-85, 2011.

[63] S. Tang, M. Allen, R. Phipps, D. Burr and D. Vashishth, "Changes in non-enzymatic glycation and its association with altered mechanical properties following 1-year treatment with risedronate or alendronate," *Osteoporos Int.,* vol. 20, no. 6, pp. 887-894, 2009.

[64] M. Allen, S. Reinwald and D. Burr, "Alendronate reduces bone toughness of ribs without significantly increasing microdamage accumulation in dogs following three years of daily treatment," *Calcif Tissue Int.,* vol. 82, no. 5, pp. 364-360, 2008.

[65] T. Mashiba, T. Hirano, C. Turner, M. J. C. Forwood and D. Burr, "Suppressed Bone Turnover by Bisphosphonates Increases Microdamage Accumulation and Reduces Some Biomechanical Properties in Dog Rib," *Journal of Boe and Mineral Research,* vol. 15, no. 4, pp. 613-20, 2000.

[66] J. Lewis, S. Radavelli-Bagatini, L. Rejnmark, J. Chen, J. Simpson, J. Lappe, L. Mosekilde, R. Prentice and R. Prince, "The effects of calcium supplementation on verified coronary heart disease hospitalization and death in postmenopausal women: a collaborative meta-analysis of randomized controlled trials.," *J Bone Miner Res.,* vol. 30, no. 1, pp. 165-175, 2015.

[67] M. Bolland, A. Grey and I. Reid, "Calcium supplements and cardiovascular risk: 5 years on," *Ther Adv Drug Saf,* vol. 4, no. 5, pp. 199-210, 2013.

[68] A. Parfitt, C. Mathews, A. Villanueva, M. Kleerekoper, B. Frame and D. Rao, "Relationships between surface, volume, and thickness of iliac trabecular bone in aging and in osteoporosis. Implications for the microanatomic and cellular mechanisms of bone loss.," *J Clin Invest.,* vol. 72, no. 4, pp. 1396-1409, 1983.

[69] I. Sernbo and J. O., "Consequences of a hip fracture: a prospective study over 1 year," *Osteoporos Int.,* vol. 3, no. 3, pp. 148-153, 1993.

[70] J. M. Kreider and S. A. Goldstein, "Trabecular Bone Mechanical Properties in Patients with Fragility Fractures," *Clin Orthop Relat Res.,* vol. 467, no. 8, pp. 1955-1963, 2009.

VITA

Drew Alexander Jones

EDUCATION:

University of Kentucky
BS Biosystems Engineering 05/14

EXPERIENCE:

Symmetry Surgical Design Engineer	06/16 - Present
ORBIS Corporation Engineering Intern	05/13-08/15
UK Biosystems Engineering Research Assistant	05/12-08/12
Preferred Tank and Tower Draftsman	06/10-08/10

AWARDS:

University of Kentucky Biomedical Engineering Research Assistance
Oaks Scholarship
Bailey Provost Scholarship